



University for the Common Good

Detection and classification of faults in pitch-regulated wind turbine generators using normal behaviour models based on performance curves

Bi, Ran; Zhou, Chengke; Hepburn, Donald M.

Published in:
Renewable Energy

DOI:
[10.1016/j.renene.2016.12.075](https://doi.org/10.1016/j.renene.2016.12.075)

Publication date:
2017

Document Version
Peer reviewed version

[Link to publication in ResearchOnline](#)

Citation for published version (Harvard):

Bi, R, Zhou, C & Hepburn, DM 2017, 'Detection and classification of faults in pitch-regulated wind turbine generators using normal behaviour models based on performance curves', *Renewable Energy*, no. 105, pp. 674–688. <https://doi.org/10.1016/j.renene.2016.12.075>

General rights

Copyright and moral rights for the publications made accessible in the public portal are retained by the authors and/or other copyright owners and it is a condition of accessing publications that users recognise and abide by the legal requirements associated with these rights.

Take down policy

If you believe that this document breaches copyright please view our takedown policy at <https://edshare.gcu.ac.uk/id/eprint/5179> for details of how to contact us.

1 **Detection and Classification of Faults in Pitch-regulated Wind Turbine Generators** 2 **Using Normal Behaviour Models Based on Performance Curves**

3 Ran Bi* , Chengke Zhou and Donald M Hepburn

4 School of Engineering and Built Environment, Glasgow Caledonian University, Glasgow, UK G4
5 0BA

6 *Corresponding author. Tel.: +44-747-249-9306; E-mail: ran.bi@gcu.ac.uk

7 Email: C.Zhou@gcu.ac.uk; D.M.Hepburn@gcu.ac.uk

9 **Highlights**

- 10 ● Propose normal behaviour models based on performance curves to detect WTG faults;
- 11 ● Examine WTG performance under the normal conditions and with pitch faults;
- 12 ● Demonstrate the feasibility of the proposed approach based on performance curves;
- 13 ● Validate the criteria for electrical pitch system fault detection;
- 14 ● Prove the advantages of the proposed approach over the ANN/ANFIS based approaches.

15 **Abstract**

16 The fast growing wind industry requires a more sophisticated fault detection approach in pitch-
17 regulated wind turbine generators (WTG), particularly in the pitch system that has led to the highest
18 failure frequency and downtime. Improved analysis of data from Supervisory Control and Data
19 Acquisition (SCADA) systems can be used to generate alarms and signals that could provide earlier
20 indication of WTG faults and allow operators to more effectively plan Operation and Maintenance
21 (O&M) strategies prior to WTG failures. Several data-mining approaches, e.g. Artificial Neural
22 Network (ANN), and Normal Behaviour Models (NBM) have been used for that purpose. However,
23 practical applications are limited because of the SCADA data complexity and the lack of accuracy due
24 to the use of SCADA data averaged over a period of 10 minutes for ANN training. This paper aims to
25 propose a new pitch fault detection procedure using performance curve (PC) based NBMs. An
26 advantage of the proposed approach is that the system consisting of NBMs and criteria, can be
27 developed using technical specifications of studied WTGs. A second advantage is that training data is
28 unnecessary prior to application of the system. In order to construct the proposed system, details of
29 WTG operational states and PCs are studied. Power-generator speed (P-N) and pitch angle-generator
30 speed (PA-N) curves are selected to set up NBMs due to the better fit between the measured data and
31 theoretical PCs. Six case studies have been carried out to show the prognosis of WTG fault and to
32 demonstrate the feasibility of the proposed method. The results illustrate that polluted slip rings and
33 the pitch controller malfunctions could be detected by the proposed method 20 hours and 13 hours
34 earlier than by the AI approaches investigated and the existing alarm system. In addition, the proposed
35 approach is able to explain and visualize abnormal behaviour of WTGs during the fault conditions.

36 *Keywords:* condition monitoring, wind turbine generator, pitch faults, performance curves, normal
37 behaviour model

38 **Abbreviation**

39	WTG	Wind Turbine Generator
40	SCADA	Supervisory Control and Data Acquisition
41	O&M	Operation and Maintenance
42	ANN	Artificial Neural Network
43	NBM	Normal Behaviour Model
44	PC	Performance Curve
45	CM	Condition Monitoring
46	ANFIS	Adaptive Neuro-Fuzzy Interference System
47	APK	A-Priori Knowledge
48	SIMAP	Intelligent System for Predictive Maintenance
49	CMS	Condition Monitoring System

1	GC	Grid Connection
2	MPPT	Maximum Power Point Tracking
3	PP	Power Production
4	ES	Emergency Shutdown
5	CS	Case Study
6	MISO	Multiple inputs and Single Output
7	DFIG	Doubly Fed Induction Generator
8	PMSG	Permanent Magnet Synchronous Generator

9

10 Nomenclature

11	n_{GCS}	The grid connection speed (rpm)
12	n_{HPS}	The highest production generator speed (rpm)
13	n_{LPS}	The lowest production generator speed (rpm)
14	n_r	The rated generator speed (rpm)
15	P_{GC}	The maximum grid connection power output (kW)
16	P_{max}	The maximum of power output (kW)
17	P_{nr}	The power output when n_r is reached (kW)
18	P_r	The rated power output (kW)
19	v_{cut-in}	Cut-in wind speed (m/s)
20	$v_{cut-out}$	Cut-out wind speed (m/s)
21	v_{nr}	The wind speed where n_r is reached (m/s)
22	v_r	The rated wind speed (m/s)
23	β_{ES}	The feathered position (deg.)
24	β_f	The setting of pitch angle under freewheeling (deg.)
25	β_{MO}	The maximum pitch angle for operation (deg.)
26	β_{PL}	The setting of pitch angle under unrated power (deg.)

27

28 1. Introduction

29 Wind turbine generators (WTG) are complex electromechanical devices that are prone to shut down
30 due to subsystem faults [1]. The annual report of the onshore wind farm in China, which has provided
31 the data for this investigation, gave the top three electrical pitch-regulated WTG fault frequencies
32 during 2014 as: pitch faults (42.26%), converter faults (31.01%) and vibration faults (7.39%). In
33 respect of these fault types, pitch faults were responsible for 34.46%, converter faults for 29.01% and
34 generator faults for 12.35% of the annual downtime during 2014. Failures of WTGs result in high
35 operation and maintenance (O&M) costs and negatively impact on operational performance [2].
36 Assessment of fault conditions, through monitoring of WTG operational data, would permit operators
37 to identify early stage deterioration and to prioritise remedial actions, essential to reduce the
38 downtime and O&M costs.

39 Condition monitoring (CM) techniques, based on vibration analysis, oil analysis and strain
40 measurement, have been widely studied, e.g. [3] and [4]. Although some have been highly effective in
41 improving the O&M practice in the field of aerospace, power systems and rotational machines, those
42 CM techniques require mounting additional sensors or devices and they focus on monitoring specific
43 aspects of a device. Due to the high cost of fitting and maintaining such systems, not all WTGs have
44 had the CM equipment installed.

45 Supervisory Control and Data Acquisition (SCADA) systems are a standard installation on large
46 WTGs monitoring and recording the operational conditions [5]. Achieved SCADA data provides
47 comprehensive signal information, historical alarms and detailed fault logs. In the design of a SCADA
48 system, fault detection and prognosis schemes are simple and are often conservative. WTGs are
49 automatically shut down even during simple faults to wait for inspection and maintenance [6].

50 Each WTG's systematic performance can be monitored through rigorous analysis of the information
51 collected by the SCADA system, using data driven model-based condition monitoring schemes [7].

1 Based on this database of information, data-mining based approaches and Normal Behaviour Models
2 (NBM) have gained popularity in research methods attempting to provide early indication of faults.
3 The NBMs are able to predict on-line reference condition parameters expected for each WTG
4 component [8], according to its current operational and environmental conditions. Deviation from the
5 expected output indicates an abnormal operational state.

6 Sanz-Bobi *et al.* [9] applied an artificial neural network (ANN) approach to develop three NBMs
7 using 10-minute averaged SCADA data, i.e. gearbox bearing temperature model, gearbox thermal
8 difference model and gearbox oil temperature model. A predictive maintenance system, Intelligent
9 System for Predictive Maintenance (SIMAP), is created for WTG gearbox condition monitoring,
10 however, the ANN based NBM is a black-box model which fits globally a single function from the
11 training data and thereby losing insight into a problem. It is disadvantageous that this model requires a
12 large amount of accurate data for training prior to application. In addition, although using time
13 averaged SCADA data may be suitable in the case of gearbox oil temperature fails. This may not be
14 effective in other areas.

15 Schlechtingen *et al.* [10] proposed a system for wind turbine condition monitoring applying Adaptive
16 Neuro-Fuzzy Interference System (ANFIS) which is a combination of the ANN and fuzzy logic
17 analysis. 45 NBMs were developed to analyse SCADA data, in this case the data had been averaged
18 over 10-minute intervals. The second part of the work illustrated some example applications of the
19 system, e.g. a hydraulic fault, cooling system fault, anemometer fault and turbine controller
20 malfunctions [11]. However, the application of the ANFIS hinged on expert supervision and the
21 expert input to the model was not provided. Moreover, researchers paid attention to data
22 characteristics associated with failure events and ignored the physical mechanisms of failures.

23 Chen *et al.* [12] applied a modified ANFIS approach, A-Priori Knowledge (APK) ANFIS, to achieve
24 automated detection of significant pitch faults, again using 10-minute averaged SCADA data. In that
25 work, variations of four SCADA signals (rotor speed, blade angle, motor torque and power output)
26 against wind speed were monitored to identify pitch faults. However, they ignored the different
27 operational characteristics between stop-to-operation process and operation-to-stop process, which is
28 key to success of the approach as will be demonstrated in the paper.

29 WTG performance curves (PC) depict the relationships among power output and other measurable
30 parameters [13]. Three different PCs, namely power-wind speed (P-V) curve, rotor speed-wind speed
31 (N_r -V) curve, and pitch angle-wind speed (PA-V) curve, were studied in [13] using 10-min averaged
32 SCADA data. Applying *k*-means clustering and Mahalanobis distance, reference PCs were obtained to
33 detect the bivariate data. As in [12], differences during different operational states were not
34 considered.

35 This paper considers whether NBMs based on PCs may be an effective tool to quantify the
36 performance and detect abnormal conditions of WTGs. When applying PC based NBMs, it is
37 important to identify reference PCs using valid physical functions. This paper aims to establish a full
38 understanding of WTG operational states and develop a set of improved NBMs for use in the
39 condition monitoring system (CMS) for WTGs based on PCs using instantaneous SCADA data (1
40 second interval). The models or PCs used in this work include power-generator speed (P-N)
41 relationship, and pitch angle-generator speed (PA-N) relationship. Knowledge of operational states
42 and pitch fault mechanism are helpful to develop PC based models and criteria for fault prognosis.

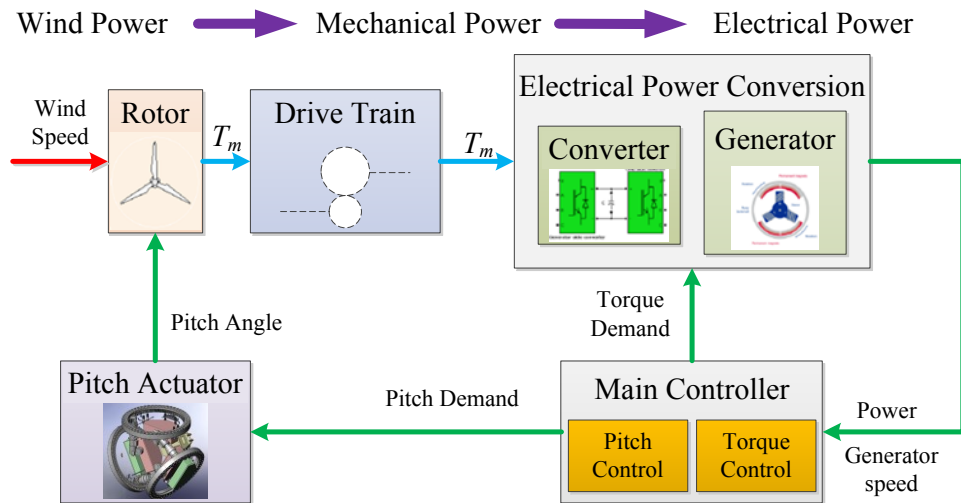
43 The paper is organized as follows. Section 2 presents a description of WTG operational states and PCs.
44 In Section 3, the pitch fault symptoms are analysed in details. Based on the findings, a set of diagnosis
45 criteria is proposed in Section 4. In Section 5 the developed method applied to pitch-regulated WTGs
46 to show its ability in detecting pitch faults and forecasting the WTG failures. The results of AI based
47 models and the existing alarm system are compared in this section.

48

1 2. Operational States and Performance Curves

2 2.1. Operational states

3 Fig. 1 illustrates the process of power conversion and the typical control loop of a pitch regulated
 4 WTG. The rotor is rotated by the wind and provides mechanical power to the drive train [14]. The
 5 drive train is a transmission system to transfer the mechanical power, P_m , and torque, T_m , to the
 6 generator. The generator produces electrical power under the influence of the converter. The main
 7 controller depends on power output and rotational speed of the generator to calculate expected pitch
 8 angle and generator torque. The pitch actuators rotate blades about their longitudinal axis to ensure
 9 the appropriate energy is extracted from the available wind power.



10

11 Fig. 1. Power conversion and control flow chart within a WTG system.

12 Fig. 1 indicates that wind speed (v), mechanical torque (T_m and T_m'), generator speed (n), pitch angle
 13 (β) and power output (P) are important measurements for assessing the efficiency of power generation
 14 and, as will be demonstrated, condition monitoring. All of the named parameters, except the torque,
 15 can be easily obtained from the SCADA system. In this work, wind speed, power output, generator
 16 speed and pitch angle are observed when different operational states are studied. It will be shown that,
 17 although wind speed shows the condition of wind, this provides too variable a signal to consider it as
 18 a monitoring tool. Power output, generator speed and pitch angle more accurately depict the
 19 behaviour of WTGs.

20 Details of the seven WTG operational states are illustrated in Fig. 2 [15]. The wind speed can be
 21 classified into five regions marked in different colours to facilitate understanding of WTG behaviour
 22 under different conditions. The operation under each condition is discussed in the next sections. It
 23 should be noted that there are three operational states for wind speeds below the cut-in wind speed
 24 (v_{cut-in}).

25 *Stationary*: When the wind speed below v_{cut-in} , i.e. the wind speed at which WTGs start producing
 26 electrical power, there are three operational states due to different conditions of the WTG. The
 27 Stationary state is characterized by a stationary rotor and engaged parking brake. Therefore the WTG
 28 is at a standstill and blades are adjusted at the feathered position, i.e. where the pitch angle is the
 29 maximum (β_{ES}) and blades are under the least stress in this stationary state. The control system
 30 ensures that the WTG is ready to operate or to get it ready to operate when the wind conditions are
 31 suitable and there is demand for power.

32 *Freewheeling*: In freewheeling state the WTG does not produce electrical power, but the generator
 33 rotor is rotating and the pitch angle is adjusted to β_f , i.e. a setting of pitch angle which allows the rotor
 34 to gain energy form the available wind. The generator speed lies in the range $(0, n_{GCS})$ and the power

1 output is 0. When the generator speed approaches n_{GCS} , the generator or converter contactor is closed
 2 and the Grid Connection state is entered.

3 *Grid Connection (GC)*: In the stop-to-operation process, the brake is released and the generator rotor
 4 accelerates up to the grid connection operating speed (n_{GCS}) when the WTG starts grid connection.
 5 Meanwhile, the pitch angle reduces from β_{ES} to a proper value for operation, as dictated by wind
 6 speed and other operational parameters.

7 The wind speed has to be higher than v_{cut-in} . Electrical power can be produced and the control system
 8 ensures a constant operating generator speed of n_{GCS} , which is a design parameter avoiding the
 9 resonance [16]. During grid connection the WTG orients into the wind all the time. In this state, the
 10 ideal condition is that generator speed is remained at n_{GCS} , and power output lies between 0 and P_{GC} ,
 11 i.e. the maximum of power output in grid connection state. When the wind speed reduces to v_{cut-in} , the
 12 WTG disconnects and enters freewheeling state.

Wind	Machine	Operational States	Control Strategies
$v < v_{cut-in}$	$n = 0$ $P = 0$ $\beta = \beta_{ES}$	Stationary	Monitoring for operation
$v \leq v_{cut-in}$	$0 < n \leq n_{GCS}$ $P = 0$ $\beta = \beta_f$	Freewheeling	
$v = v_{cut-in}$	$n = n_{GCS}$ $0 \leq P < P_{GC}$ $0 < \beta < \beta_f$	Grid connection	Constant speed control
$v_{cut-in} < v < v_{nr}$	$n_{GCS} < n < n_r$ $P_{GC} \leq P < P_{nr}$ $\beta = \beta_{PL}$	Power production 1	MPPT
$v_{nr} \leq v \leq v_r$	$n = n_r$ $P_{nr} \leq P < P_r$ $\beta = \beta_{PL}$	Power production 2	Constant speed control
$v_r < v < v_{Cut-out}$	$n = n_r$ $P = P_r$ $\beta_{PL} < \beta < \beta_{MO}$	Power production 3	Constant power control
$v > v_{Cut-out}$	$n \rightarrow 0$ $P \rightarrow 0$ $\beta \rightarrow \beta_{ES}$	Emergency Shutdown	Protection

13

14 Fig. 2. Typical operational states of a pitch regulated WTG.

15 *Power Production 1 (PPI)*: Controller tasks depend on the wind velocities and operational conditions
 16 of the WTG [15]. When the wind speed is between v_{cut-in} and v_{nr} at which the generator reaches rated
 17 speed (n_r), the Power Production 1 (PP1) state is entered. The WTG functions to capture as much
 18 wind power as possible. To do this maximum power point tracking (MPPT) is applied to control the
 19 system operation. In this state, the generator speed is monotonically increasing with wind speed and
 20 lies in the range (n_{GCS} , n_r). The rotor blade pitch angles are fixed at β_{PL} , a pitch setting for partial
 21 power output. According to the similarity law in the fluid mechanics [17], the power output can be
 22 expressed as:

23
$$P = (P_{nr} / n_r^3) n^3 \quad (1)$$

24 Where P_{nr} is the power output when generator speed reaches the rated (kW); n_r is the rated generator
 25 speed (rpm).

26 *Power Production 2 (PP2)*: In PP2 wind speed lies in the range (v_{nr} , v_r), and constant speed control is
 27 used to limit the generator speed [15]. The generator rotor current can be controlled through a

1 converter to regulate the generator electromagnetic torque against the aerodynamic torque, and the
2 power output continues to increase [18]. Therefore, generator speed maintains at n_r , and the power
3 output lies in the range (P_{nr} , P_r) in ideal conditions. The pitch angle should be maintained at β_{PL} until
4 the wind speed reaches the rated value (v_r).

5 *Power Production 3 (PP3)*: Constant power control is employed when the wind speed lies between
6 the rated (v_r) and the cut-out wind speed ($v_{cut-out}$). Not all the wind power can be converted to electrical
7 power due to limitation of the generator rating. The blade pitch control is activated in this mode [14].
8 Due to the constant generator speed, the electromagnetic torque is controlled to balance with
9 mechanical torque, T_m . When the wind speed increases, the pitch angle increases to reduce the
10 mechanical torque in order to maintain the generator speed and power output. In the ideal condition,
11 generator speed is n_r ; power output is P_r ; and pitch angle lies between β_{PL} and β_{MO} , the maximum
12 pitch angle for all operational states.

13 *Emergency Shutdown (ES)*: ES state is entered due to emergency conditions where the wind speed
14 exceeds $v_{cut-out}$. In this state, an operation-to-stop process is carried out. Pitch angle increases to the
15 feathered position at the maximum velocity. The generator speed reduces to zero and, hence, the
16 power output also reduces to zero. The emergency conditions involve when the normal shutdown
17 procedure is deemed too slow to protect the WTG or when the normal shutdown is deemed ineffective
18 due to a component failure.

19 2.2. Performance curves

20 There are five PCs for observation: power-wind speed (P-V) curve, generator speed-wind speed (N-
21 V) curve, pitch angle-wind speed (PA-V) curve, power-generator speed (P-N) curve and pitch angle-
22 generator speed (PA-N) curve. Due to the linear relationship between the rotor speed and generator
23 speed, N-V and N_r -V curves have same characteristics. The P-V, N-V and PA-V curves are
24 previously studied in literature, e.g. [13], and the other two P-N and PA-N are novel.

25 Using four days' of WTG operational data, which was made available to the authors, Fig. 3 shows
26 examples of the five PCs of a DFIG-WTG. It should be noted that, despite existing monitoring
27 systems being in operation, during the four days, the WTG was never shut down due to any fault.

28 The relevant technical specifications of the WTG studied are shown in Table A (CS1): these were
29 used to construct the theoretical PCs. It is noted that v_{nr} and P_{GC} which are used to separate the
30 operational states of the WTG cannot be obtained exactly. The theoretical PA-N curve of three PP
31 states and the theoretical P-N curve are shown as a solid red line in Fig. 3(d) and (e).

32 A P-V curve indicates power generated by a WTG at various wind velocities, as shown in Fig. 3. A
33 typical P-V curve resembles a sigmoid function; however, malfunctions of a WTG will impact its
34 power generation [13]. Deviation from the theoretical line will also occur if there are variations in
35 wind speed and wind direction which are not responded to by the control mechanism due to inertia of
36 the system or rate of change differences.

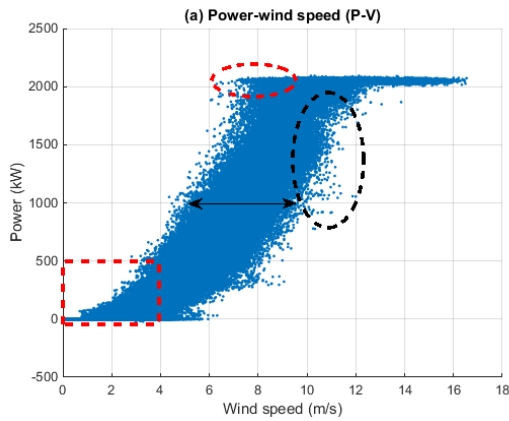
37 In Fig. 3, the measured data circled by the red dashed rectangle shows that there is positive power
38 output when the measured wind speed is lower than the cut-in wind speed (4 m/s) due to the rotor
39 inertia and constant speed control in grid connection state [19]. When the wind speed reduces to
40 around v_{cut-in} , for short periods of time the generator speed maintains at n_{GCS} , and the GC state is
41 maintained. Similarly, the data circled by the dashed red ellipses is related to when wind speed falls
42 below the rated speed, v_r , and the dashed black ellipse is indicative of when wind speed increases over
43 v_r . In Fig. 3, the double arrowed line shows that the variation of the wind speed of nearly 4 m/s, a
44 constant power output of 1000 kW is remained. From this information, the wind speed does not
45 correlate well with the power output and so variation within the P-V curve would be unreliable as an
46 indicator of fault conditions.

47 An N-V curve represents the mapping between rotor speed and wind speed, as shown in Fig. 3(b).
48 Failures of turbine components can change the shape [13]. The double arrowed line shows that the

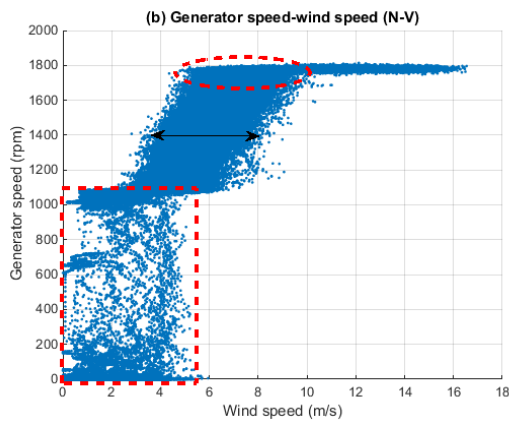
1 variation of the wind speed is nearly 4 m/s at a constant generator speed of 1400 rpm. The data in the
 2 red rectangle illustrates that the generator may still rotate when wind speed is lower than v_r . When the
 3 wind speed reduces to the cut-in wind speed and further reduces, the change in the generator speed
 4 lags the wind speed due to the inertia of the rotor [19]. The red circled data demonstrates a similar
 5 relationship, i.e. as a result of inertia the generator speed will remain the rated value despite the wind
 6 speed falling below rated value. Combining the analysis of Fig. 3(a) and (b), it is found that the two
 7 constant speed control regions have boundary of ± 2 m/s around v_{cut-in} and v_r respectively.

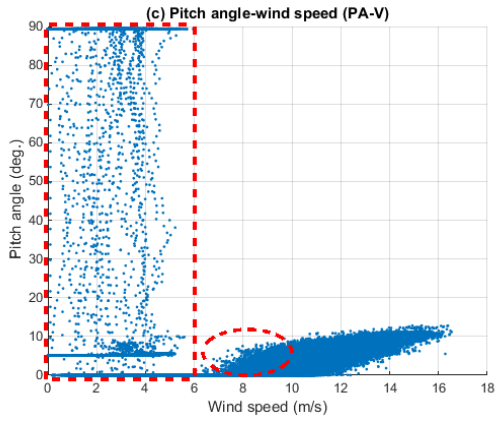
8 A PA-V curve shows the relationship between the blade pitch angle and wind speed, as shown in Fig.
 9 3(c). Different designs of the pitch control systems result in different characteristics of the pitch angle
 10 [13][20]. Generally, the pitch angle is increased to reduce the wind power captured by the turbine [13]
 11 when wind speed is above a certain threshold. When wind speed reduces to below v_{cut-in} , the pitch
 12 angle is adjusted to the feathered positions [12], as shown in red rectangle. When the wind speed lies
 13 between v_{cut-in} of 4 m/s and v_r of 10 m/s, the pitch angle should be maintained at β_{PL} of 0° . However, in
 14 the red ellipse the pitch angle is higher than 0° . The poor relationship in the ellipse region is also
 15 shown through the remainder of the wind speed range: this is likely to be because pitch angle cannot
 16 change as quickly as the wind speed.

17

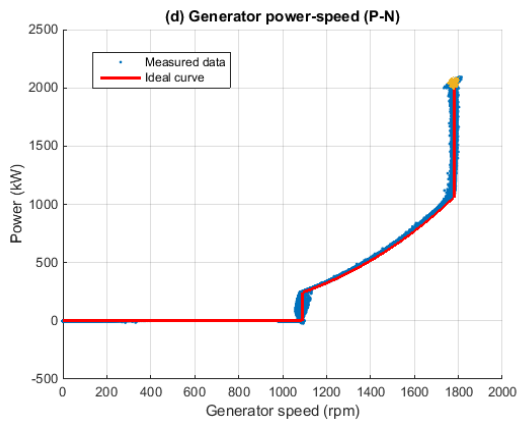


18

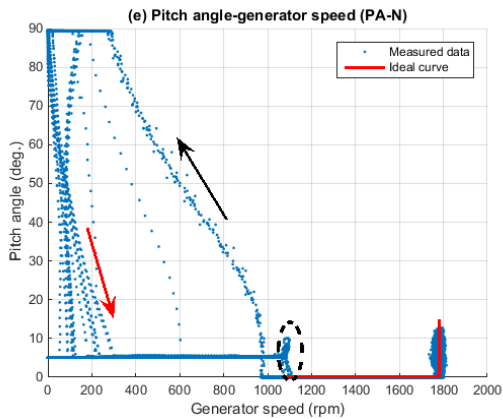




1



2



3

4 Fig. 3. Relationships using SCADA data of a DFIG-WTG in normal conditions: (a) P-V; (b) N-V; (c)
5 PA-V; (d) P-N; (e) PA-N.

6 The three PCs outlined above, all related to wind speed, have been used to study the operational
7 behaviour of WTGs in [13]. However, as demonstrated above using real world data, these measured
8 values have a large spread over the theoretical curves, due to the practical reaction times of the
9 various system components. As discussed in [19], they cannot be relied on to model the theoretical
10 relationship between the measurements and wind speed due to the rotor inertia.

11 A P-N curve, which illustrates the relationship between the power output and generator speed, is
12 shown in Fig. 3(d). It can be seen that the measured data fit the theoretical curve, indicated by the
13 solid line, significantly better than previous PCs.

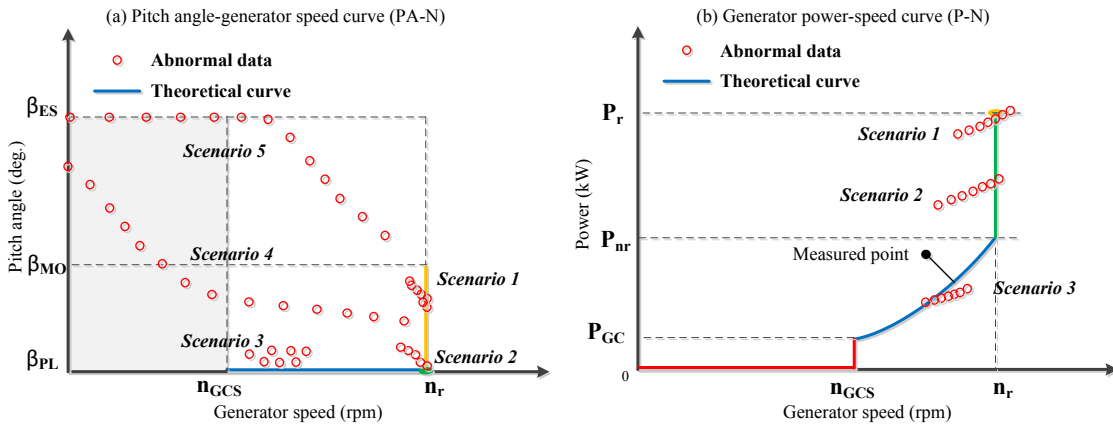
14 A PA-N curve, which depicts the variation of pitch angle at different generator speed, is illustrated in
15 Fig. 3(e). The characteristics of the pitch angle can be easily analysed in all three PP states and they

1 are corresponding to the theoretical analysis. When a shutdown occurs, pitch angle increases to the
 2 feather position of 90 degree and generator speed reduces below n_{GCS} , as shown following the black
 3 arrow. When the stop-to-operation process is going on and the WTG changes from Stationary state to
 4 Freewheeling state: following the red arrow, pitch angle are adjusted to β_f and generator speed
 5 increases. The black eclipse shows the GC state. It is seen that only in three PP states the PA-N
 6 relationship can be relied on to model, as shown in Fig. 3(e).

7 In comparisons among the five PCs, P-N and PA-N curves show better consistency when fitting the
 8 measured data to the theoretical values and the variation from the curve under normal operational
 9 states is low. Therefore, a set of criteria can be established using envelopes around the PCs under
 10 normal conditions. Any deviations from the envelopes indicate a WTG pitching faults. Any pitch
 11 controller malfunction and slip ring pollution, critical failure modes of WTGs, results in that the pitch
 12 angle does not meet expectations and causes wind power extraction to differ from normal operational
 13 conditions [19].

14 3. Analysis of Pitch Faults and Change to the PCs

15 Slip ring pollution and pitch controller malfunction are two dominant causes to pitch faults in
 16 electrical pitch systems of WTGs [1]. The slip ring mounted between the rotor and the nacelle to
 17 deliver the control signals, data and electrical power. Polluted slip ring causes poor communication
 18 and pitching malfunction. The pitch controller malfunction directly sends wrong command to pitch
 19 actuators.



20 Fig. 4. Ideal curves and abnormal data: (a) PA-N curve; (b) P-N curve.

22 By comparing and analysing the difference between normal conditions and the WTG fault periods in
 23 different operational states, 2D views of PCs can be used to identify WTG pitch faults. Fig. 4
 24 illustrates the theoretical P-N and PA-N curves and also the scenarios when pitch control system
 25 malfunctions. The measured data point deviate from normal PCs, and therefore the distance between
 26 the point and the curve can be used as an indicator to identify the abnormal data and detect faults. It is
 27 noted that the abnormal data only means it has different relationship from the normal values.

28 *Scenario 1:* This scenario occurs when the WTG operates at pitch fault condition in PP3 state. The
 29 pitch fault results in that the pitch angle is higher than the expected. It reduces the mechanical torque
 30 and decelerates the generator speed. Therefore, the measured data deviates to the left from the ideal
 31 PA-N curve in Fig. 4(a). Due to the reduction of generator speed, the generator torque will increase to
 32 remain the power output that equals to the product of generator speed and torque. Increasing generator
 33 torque will further decelerate the generator speed so that the WTG cannot operate in PP3 state. The P-
 34 N relationship also differs from the theoretical PA-N curve, because the power output and generator
 35 speed cannot be remained at yellow point, as shown in Fig. 4(b). If the pitch fault results in that the
 36 pitch angle is lower than the expected, Scenario 1 will develop following the opposite direction.
 37 Power output and generator speed may exceed their operational ranges.

1 *Scenario 2:* This scenario would occur when the WTG operates under PP2 with a pitch fault, as
 2 shown in Fig. 4. The characteristics of measurements are similar with Scenario 1. When the pitch
 3 angle is higher than the expected due to a pitch fault, the generator torque will reduce to balance the
 4 reduced mechanical torque and to remain the generator speed. The power output reduces due to the
 5 reduced generator speed and torque, as shown in Fig. 4(b). If the pitch fault results in that the pitch
 6 angle is lower than the expected, Scenario 2 will develop following the opposite direction and
 7 generator speed may exceed the operational range.

8 *Scenario 3:* If a pitch fault occurs when the WTG operates under PP1, Scenario 3 occurs as shown in
 9 Fig. 4. The generator speed would not reach the rated value, and the pitch angle should be β_{PL} to
 10 capture the maximum wind power. Because the pitch angle is higher than β_{PL} , the power captured by
 11 the rotor would not reach maximum, and the power output will be lower than the expected. Hence, the
 12 measured data locates below the ideal P-N curve, as shown in Fig. 4(b).

13 *Scenario 4:* This scenario occurs during the start-to-operation process, as shown in Fig. 4(a). When
 14 the wind speed is higher than v_r , WTGs will directly enter the PP3 after grid connection. It explains in
 15 this case, why the pitch angle is higher than 0 degree when the generator speed lies between n_{GCS} and
 16 n_r , as shown in Fig. 4(a).

17 *Scenario 5:* This scenario occurs during the emergency shutdown state (operation-to-stop), as shown
 18 in Fig. 4(a). When emergency conditions occur, e.g. detected fault conditions or over cut-out wind
 19 speed, pitch angle increases to β_{ES} with the maximum velocity. In the normal shutdown state, the
 20 WTG operates from PP1 state to GC state and then to Stationary state due to below the cut-in wind
 21 speed.

22 In the fault analysis of electrical pitch systems, the P-N and PA-N relationships both differ from the
 23 theoretical curves when the WTG operates at a pitch fault condition. The pitch fault can lead to
 24 abnormal behaviour of the pitch angle [12]. Therefore, the PA-N relationship should follow the
 25 theoretical PA-N curve when the WTG operates under non-fault conditions. It is noted that Scenario 4
 26 and 5 depict the behaviour that relates to the safe protection of WTG operations, but the data also
 27 deviates from the theoretical curve. In order to avoid false alarm, these two scenarios still need to be
 28 considered.

29 **4. NBMs and Criteria for Pitch Fault Detection**

30 *4.1. Normal behaviour models based on performance curves*

31 The measured data indicates that the theoretical curve will not exist in the real world they cannot fit
 32 the ideal curve perfectly. The distance between the measured data and theoretical P-N curve can be
 33 used to estimate how far the data deviates from the ideal condition. When the normal locations of the
 34 measured data is identified in P-N and PA-N diagrams, normal behaviour models (NBMs) can be set
 35 up to detect pitch fault conditions. The deviation D that is a Euclidean distance between the measured
 36 data and theoretical PCs is applied to detect pitch faults.

37 Due to the lack of a unified scale across different variables, the wind speed, generator speed and
 38 power output are normalized to their rated values. The pitch angle is normalized to the angle of the
 39 feathered position.

40 The value D_{Pn_i} is defined as the distance between the i th normalized data and its nearest point on the
 41 P-N curve:

$$42 \quad D_{Pn_i} = \left\{ \sqrt{(n_i - n)^2 + (P_i - P)^2}, (n, P) \in C_{P-N} \right\}_{\min} \quad (2)$$

43 Where C_{P-N} is a set of points which locate on the reference curve; n is generator speed and P is power
 44 output.

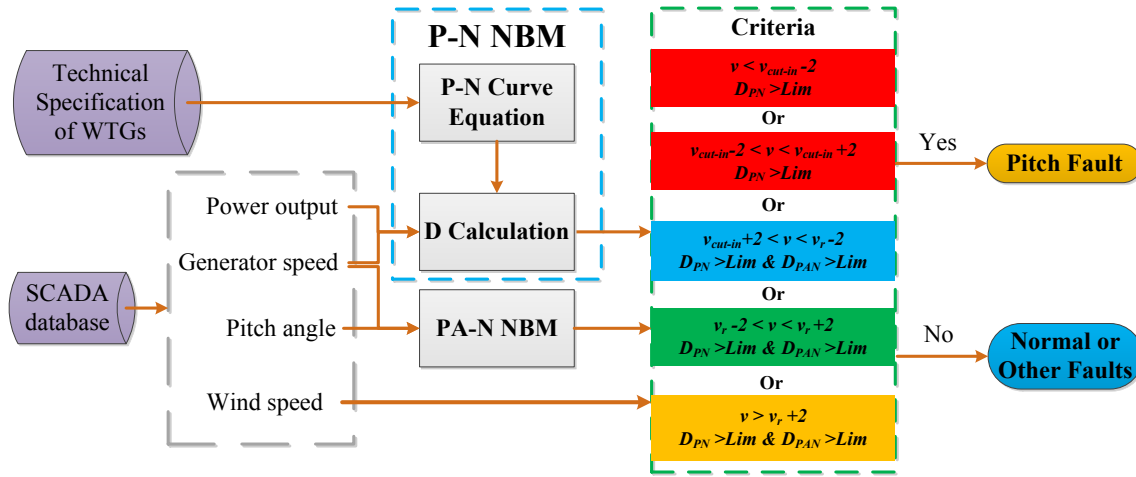
1 The value D_{PANi} is defined as the distance between the i th normalized data and its nearest point on the
 2 PA-N curve:

$$3 \quad D_{PANi} = \left\{ |1 - n_i|, |\beta_i| \right\}_{\min} \quad (3)$$

4 Using the P-N NBM and the PA-N NBM, every set of operational data produces a D_{PN} and a D_{PAN} .
 5 Therefore, NBMs can be tracked during operation every second.

6 4.2. Criteria for pitch fault detection

7 Based on the two selected NBMs a condition monitoring system (CMS) can be set up to detect WTG
 8 pitch faults. Fig. 5 illustrates the configuration of the system, which consists of a P-N NBM and a PA-
 9 N NBM with the proposed criteria. The wind speed is only used to classify the operational states, and
 10 the generator speed, pitch angle and power output are used to calculate the deviation. D_{PN} and D_{PAN}
 11 are defined as the deviation from the P-N curve and the PA-N curve respectively. If D_{PN} and D_{PAN}
 12 lie out with the normal ranges, the WTG can be regarded as being under pitch fault conditions by the
 13 system.



14
 15 Fig. 5. The configuration of NBMs based CMS of WTGs.

16 Fig. 6 shows the operational ranges on P-N curve during different operational states. It is helpful to
 17 understand the criteria introduced next. In the freewheeling state, wind speed is smaller than $(v_{cut-in}-2)$.
 18 Power output should be maintained at 0, but the WTG may produce negative power output because
 19 the auxiliary equipment is supplied by the grid, shown as point A in Fig. 6. The maximum value of
 20 the negative power output is P_{MN} that can be found in technical specifications. The thresholds can be
 21 expressed as:

$$22 \quad \lim_{D_{PN}} = \frac{|P_{MN}|}{P_r} \quad (4)$$

23 In the GC state, wind speed lies in the interval of $(v_{cut-in}-2, v_{cut-in}+2)$. During the GC state, the lowest
 24 generator speed for power production is n_{LPS} , shown as point B in Fig. 6. When the WTG cannot
 25 maintain above this generator speed, it has to disconnect to the grid. The thresholds can be identified
 26 as:

$$27 \quad \lim_{D_{PN}} = \frac{|n_{LPS} - n_{GCS}|}{n_r} \quad (5)$$

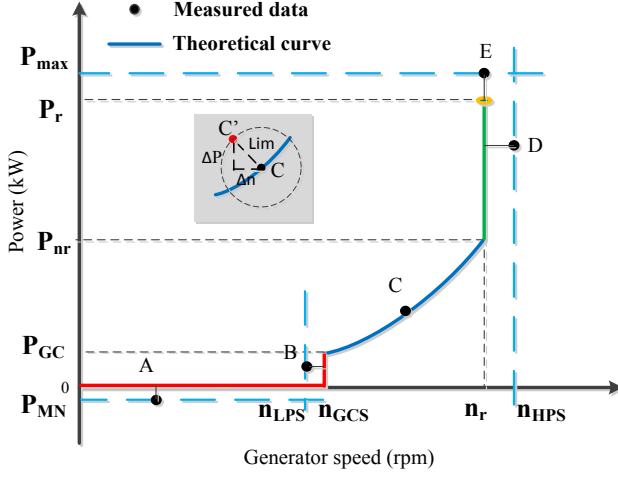


Fig. 6. The operational ranges of power output and generator speed during different operational states.

In the PP1, wind speed belongs $(v_{cut-in}+2, v_r-2)$. The generator speed is controlled to follow maximum wind power capture. The fluctuation of generator speed and power output is within 1.5% of rated values. The pitch angle is not higher by more than 1 degree. As shown in Fig. 6, if the generator speed and power output both have the maximum fluctuations, the deviation between the C' and C should be the threshold for normal operation. The thresholds can be set as:

$$\begin{cases} \lim_{D_{PN}} = \sqrt{\Delta n^2 + \Delta P^2} = 0.015 \times \sqrt{2} = 0.02 \\ \lim_{D_{PAN}} = 1 / \beta_{ES} \end{cases} \quad (6)$$

In the PP2, wind speed belongs (v_r-2, v_r+2) , shown as the point D in Fig. 6. Considering the transition between the fixed and variable pitch angle, the threshold of PA-N is set at the middle of thresholds in PP1 and 3.

$$\begin{cases} \lim_{D_{PN}} = |n_{HPS} - n_r| \\ \lim_{D_{PAN}} = \frac{1 / \beta_{ES} + |n_{HPS} - n_r|}{2} \end{cases} \quad (7)$$

In the PP3, wind speed is higher than (v_r+2) . The highest production generator speed for grid connection is n_{HPS} and the highest production power output is P_{max} , shown as the point E in Fig. 6. Due to the constant control strategy, the deviation cannot be more than the difference between the rated and the maximum value in normal conditions. The thresholds can be expressed as:

$$\begin{cases} \lim_{D_{PN}} = \{|n_{HPS} - n_r|, |P_{max} - P_r|\}_{\min} \\ \lim_{D_{PAN}} = |n_{HPS} - n_r| \end{cases} \quad (8)$$

There are two scenarios where the system cannot be regarded in abnormal conditions. One is the start process, shown as Scenario 4 in Fig. 4(b).

$$\begin{cases} n_{i-4} \leq n_{i-3} \leq n_{i-2} \leq n_{i-1} \leq n_i \\ \beta_{i-4} \geq \beta_{i-3} \geq \beta_{i-2} \geq \beta_{i-1} \geq \beta_i \end{cases} \quad (9)$$

Equation (9) depicts this criterion: when generator speed continuously increases and pitch angle continuously reduces for 5 seconds, the WTG is starting for operation. If the WTG operates in all PP states, generator speed and pitch angle will seldom monotonously vary.

1 The other is the shutdown state. Similarly, it can be expressed as:

$$2 \quad \begin{cases} n_{i-4} \geq n_{i-3} \geq n_{i-2} \geq n_{i-1} \geq n_i \\ \beta_{i-4} \leq \beta_{i-3} \leq \beta_{i-2} \leq \beta_{i-1} \leq \beta_i \end{cases} \quad (10)$$

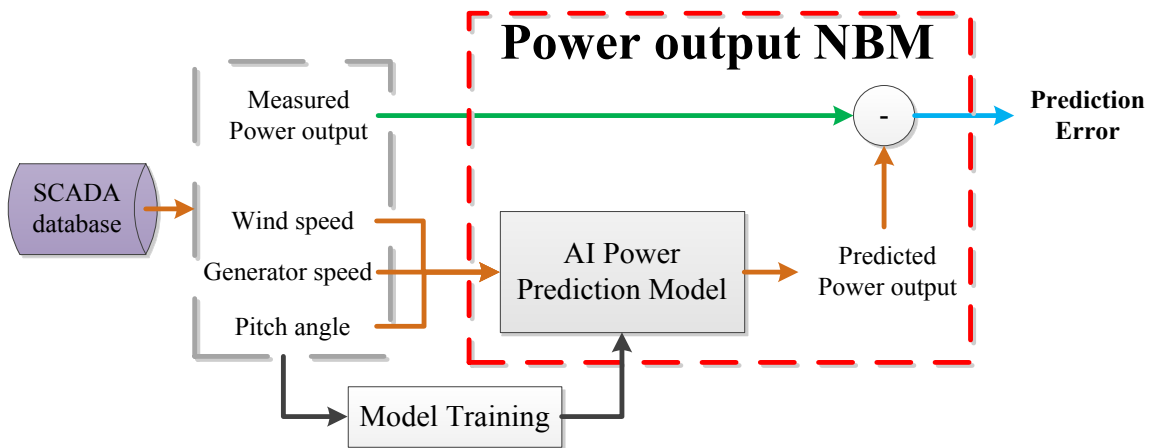
3 Or when the pitch angle exceeds the β_{MO} , the WTG enters the shutdown state due to emergency
4 conditions.

5 4.3. Normal Behaviour Models Based on ANN and ANFIS

6 AI approaches considering wind speed, generator speed and pitch angle are able to predict the
7 expected power output of a WTG under different input parameters. These trained models are used to
8 set up power output NBMs, as shown in Fig. 7. The inputs of this MISO NBM include measured wind
9 speed, power output, generator speed, and a trained AI power prediction model. This NBM output
10 allows a prediction error between predicted and measured power output to be determined with a set of
11 input parameters.

12 During normal operations the prediction error should be around zero. Any fault related to input
13 parameter, such as measurement errors, pitch system faults, and generator faults may lead to
14 differences between measured and predicted power output.

15 The settings and training processes of the ANN to predict power output of a WTG can refer to [20].
16 Similarly, the settings and training processes of the ANFIS can refer to [10].



17
18 Fig. 7. A configuration of a power output NBM of a WTG using AI approaches.

19 5. Case Studies and Discussion

20 In order to demonstrate the feasibility of the proposed CMS, six case studies have been carried out to
21 demonstrate the prognosis of pitch faults. Results were compared to the existing condition monitoring
22 and alarm system which caused the WTG shutdowns. Results of AI based NBMs are also compared in
23 this section.

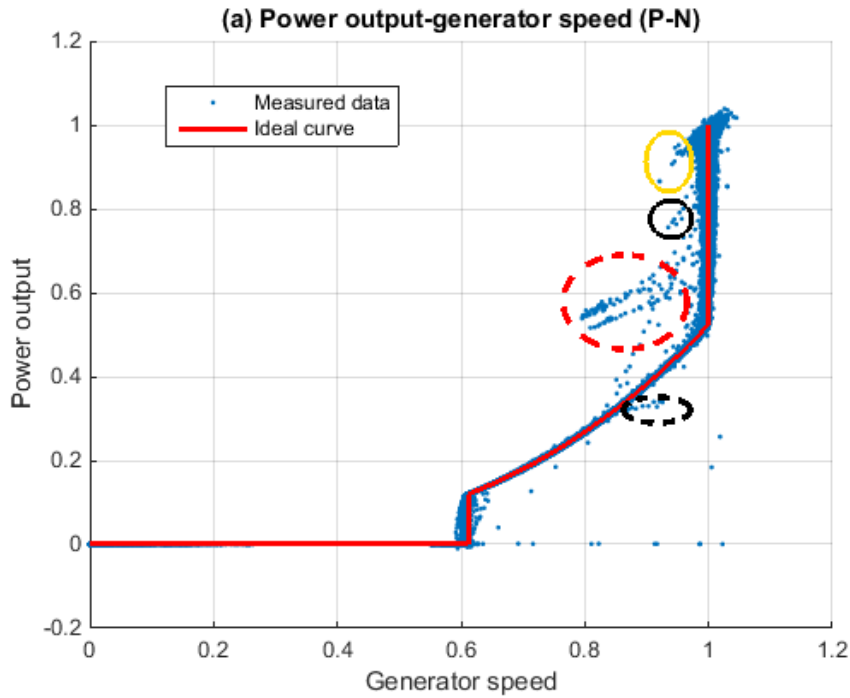
24 5.1. Case study 1 – slip ring pollution of a DFIG-WTG

25 In this case a WTG alarmed a pitch system fault and entered the emergency shutdown state at 5 am on
26 3/Mar/2015. After the inspection of the pitch system, maintenance personnel diagnosed that a polluted
27 slip ring was the cause of the failure.

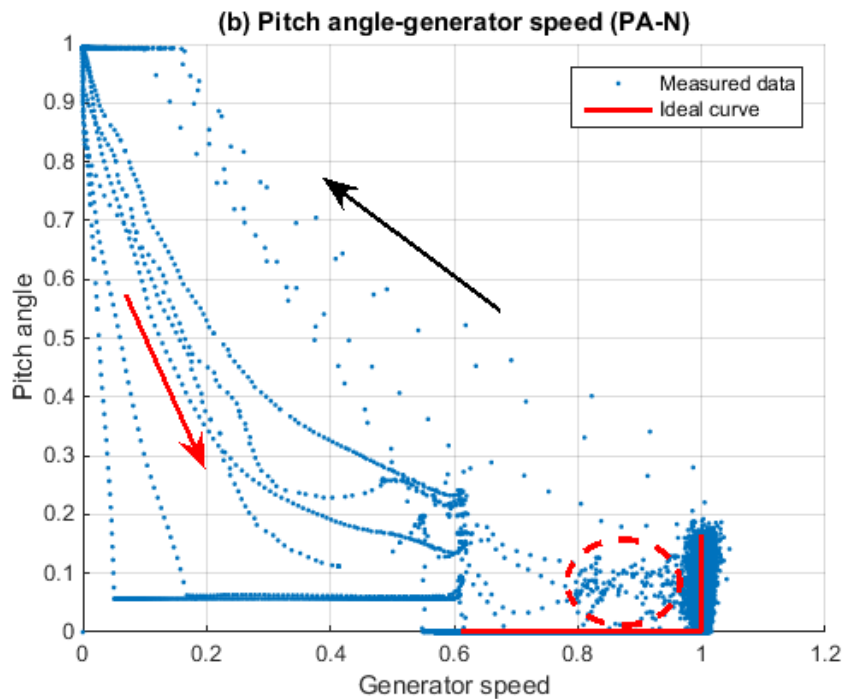
28 The polluted slip ring caused the poor communication between the pitch actuators and the main
29 controller. The pitch angle could not change because the pitch actuators do not receive any command.
30 After the maintenance on the slip ring, the WTG continued operating and no faults were alarmed.

1 Except the warnings that the wind speed was not available for the WTG to operate in power
 2 production, there was no warning of any fault prior to the WTG shutdown.

3 During the period, there were 292,693 sets of instantaneous SCADA data, each set of which contains
 4 a wind speed, a power output, a generator speed and a pitch angle. The instantaneous SCADA data of
 5 the WTG operating between 28 February 2015 and 3 March 2015 were collected to analyse, and
 6 investigate the behaviours of the WTG during this period prior to shut down. The 2D views of
 7 measured P-N and PA-N curves are shown in Fig. 8.



8



9

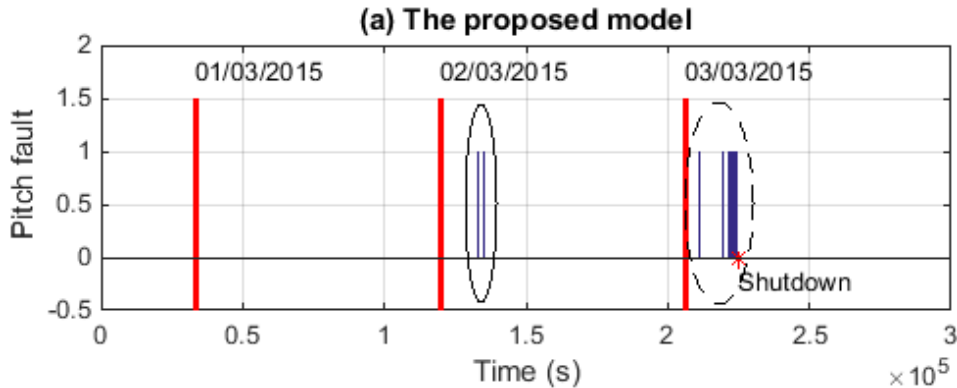
10 Fig. 8. 2D views of selected performance curves in Case Study 1: (a) P-N; (b) PA-N.

1 Generator speed and power output reduced following Scenario 1, as circled in yellow solid line in Fig.
 2 8(a). At the same time, the pitch angle lies in the red dashed circle in Fig. 8(b). There are 19 sets of
 3 data collected from 3:35:37 on 2/Mar/2015 in this Scenario. These data sets clearly deviate from the
 4 ideal curves. Next, when wind speed varied around V_r , the power output cannot reach the rated value
 5 because the pitch angle is higher than the expected, as circled in black solid line in Fig. 8(a). Fig. 8(b)
 6 shows the pitch angle delayed to change and generator speed reduced below the rated, and therefore
 7 the data located in the dashed circle.

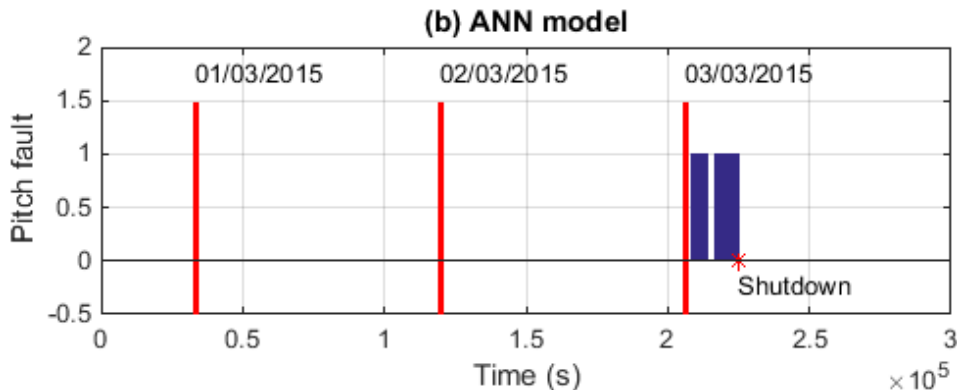
8 Scenario 2 and 3 occurred and 80 sets of abnormal data were regarded in pitch fault conditions, as
 9 shown in Fig. 8. The abnormal data following the Scenario 2 is circled by red dash line and the
 10 abnormal data following the Scenario 3 is circled by black dash line.

11 Relevant technical specifications of this DFIG-WTG are shown in Table A (CS1). Therefore, the PC
 12 based NBMs and relevant criteria can be observed. The proposed system marked the time containing
 13 abnormal data as 1 to illustrate the pitch fault condition, as circled by black solid line in Fig. 9(a). The
 14 results of AI predictions are shown in Fig. 9(b) and (c).

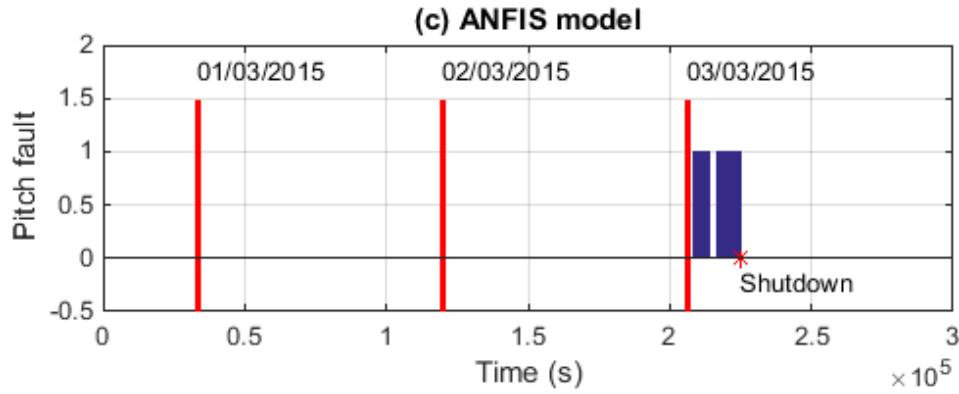
15 It is observed that the proposed system can detect the pitch fault conditions nearly 25.4 hours (91,463
 16 seconds) earlier than the existing alarm system, as shown in Fig. 9(a). ANN and ANFIS model are
 17 able to detect the abnormal data 16,177 and 17,740 second respectively earlier than the existing alarm
 18 system. As shown in Fig. 9(b) and (c), the AI models only detected the anomalies on 03/March/2015.
 19 Compared with the results of three models, the proposed system also can detect the pitch fault
 20 condition 20 hours earlier than the AI models.



21



22



1

2 Fig. 9. Comparisons of alarms using different CM techniques in Case Study 1: (a) the proposed
3 system; (b) ANN; (c) ANFIS.

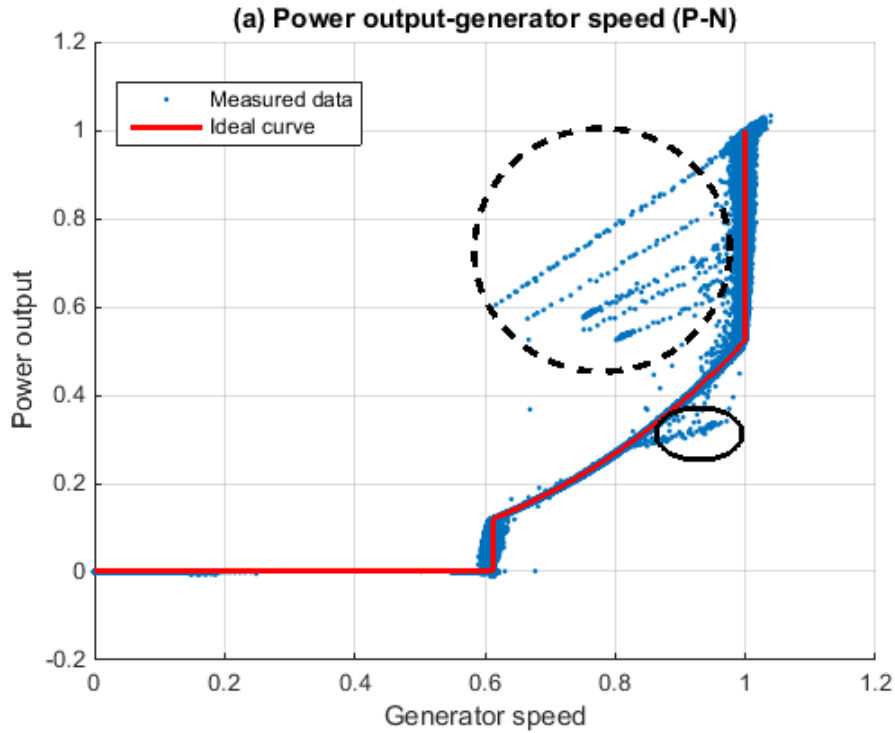
4

5 *5.2. Case study 2 – pitch controller malfunction of a DFIG-WTG*

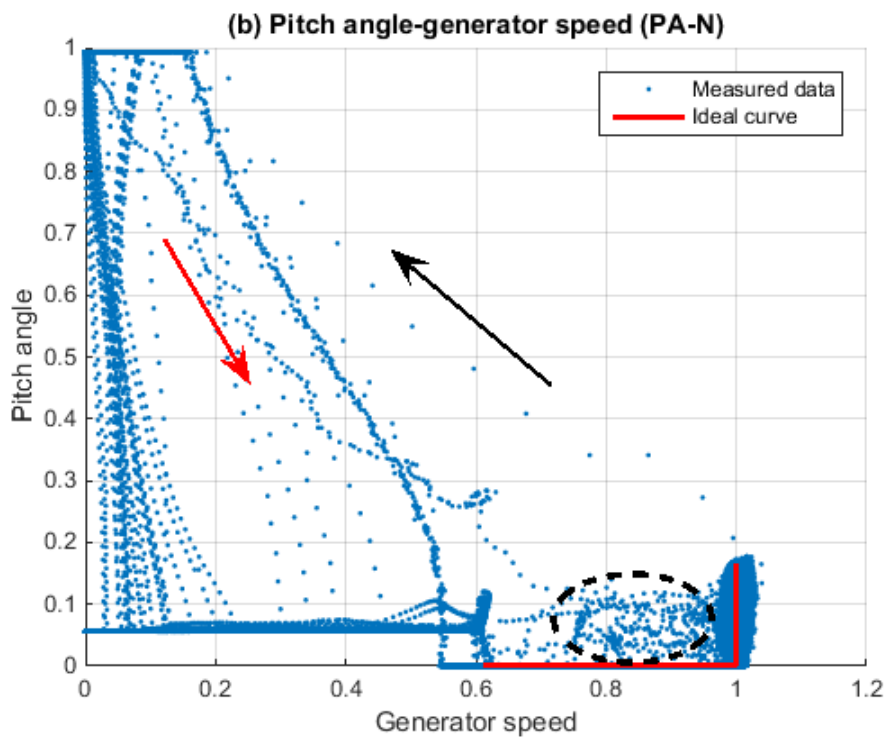
6 In this case a WTG was shut down because a scheduled inspection to pitch system was carried out at
7 20:09 on 9/Mar/2015. After inspection and updating the program of the pitch controller, the WTG
8 continued operating and no faults were alarmed. Prior to the maintenance, no pitch fault was alarmed
9 by the existing CMS but the pitch controller malfunction produced wrong signals and sent to pitch
10 actuators to move blades.

11 345,600 sets of the four measurements of the WTG operating between 6/Mar/2015 and 9/Mar/2015
12 were recorded to show behaviours of the WTG. The measured P-N and PA-N curves using
13 normalized data of the WTG are illustrated in Fig. 10. 202 sets of data were regarded as abnormal
14 data because they deviate far from the ideal curves.

15 At 18:47:37 on 8/Mar/2015 the proposed system firstly detected 66 sets of abnormal data. In this
16 period the WTG operated under PP2 state and the pitch controller malfunction occurred. The pitch
17 angle should be maintained at zero degree in this period, but the controller malfunction led to a
18 positive pitch angle. Therefore, Scenario 3 was manifested, i.e. power output is lower than the
19 expected, shown as black solid circle in Fig. 10(a). The PA-N curve shows some pitch angles are not
20 zero when the generator speed is lower than the rated, as shown in black dashed circle of Fig. 10(b).
21 Scenario 1 and 2 took place from 12:59:51 on 9/Mar/2015, and there were 136 sets of abnormal data
22 in this period, shown in black dashed circle of Fig. 10.



1

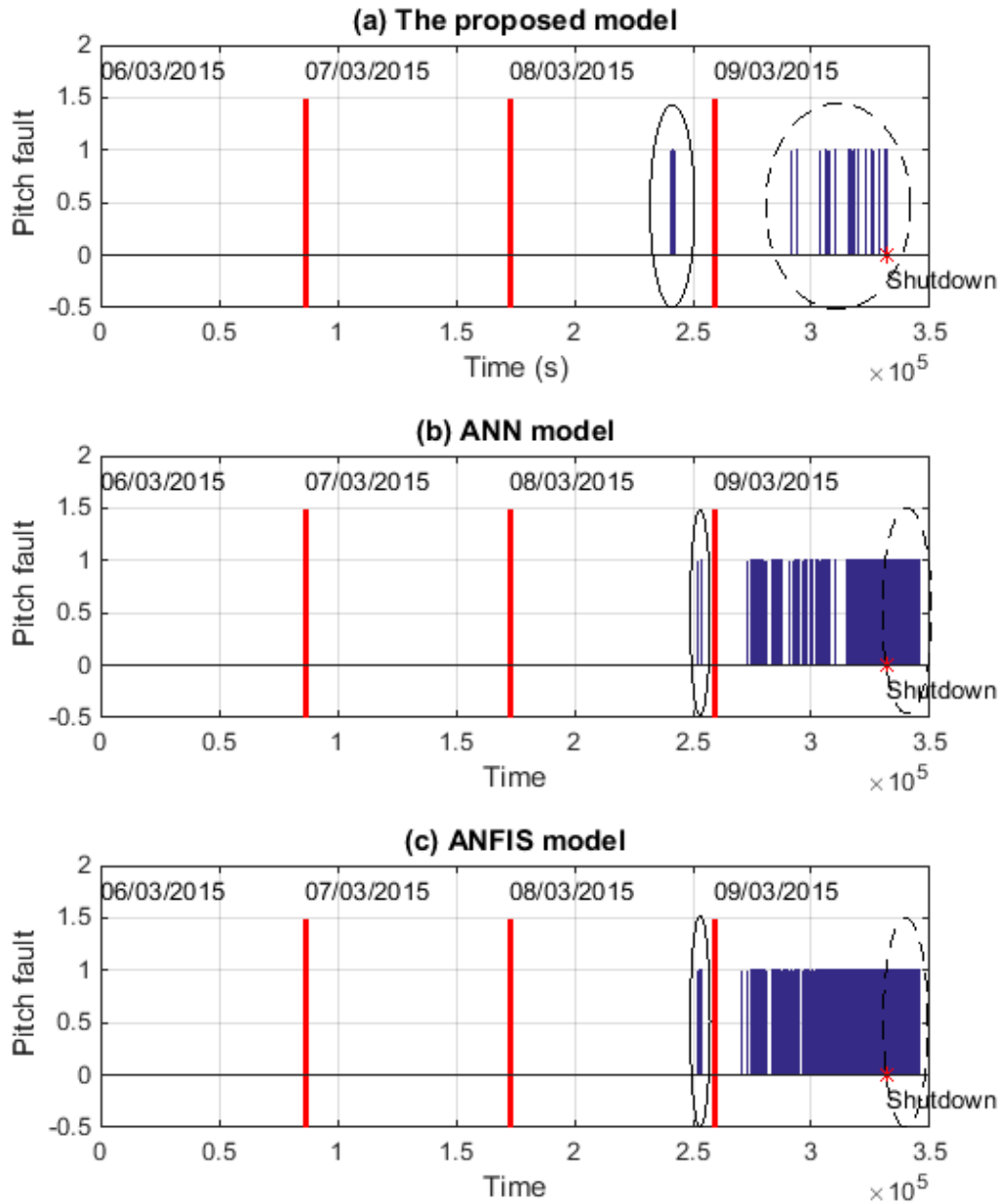


2

3 Fig. 10. 2D views of selected performance curves in Case Study 2: (a) P-N; (b) PA-N.

4 This DFIG-WTG has the same configuration and technical specifications as the WTG of Cased study
 5 1. Therefore, the PC based NBMs and relevant criteria can be observed using the same values. The
 6 analysis results of the proposed system, ANN model and ANFIS model are shown in Fig. 11. In Fig.
 7 11(a), the solid and dash circles respectively show the times when the abnormal data has been shown
 8 in Fig. 10, because the thresholds of Equation (7) and (8) were exceeded respectively.

1 It is seen that the proposed system can detect the pitch fault conditions nearly 25.3 hours (91,283
 2 seconds) earlier than the existing alarm system as marked by the red star in Fig. 11. ANN and ANFIS
 3 models can detect the abnormal data 11,235 and 11,206 seconds later than the proposed system
 4 respectively, as shown in the solid circle in Fig. 11(b) and (c). In addition, the AI approaches lack of
 5 ability to explain the prediction error. During the Stationary state after emergency shutdown (13,879
 6 sets of data), as illustrated in dash circles in Fig. 11(b) and (c), the prediction errors exceed the
 7 limitation.



8

9

10

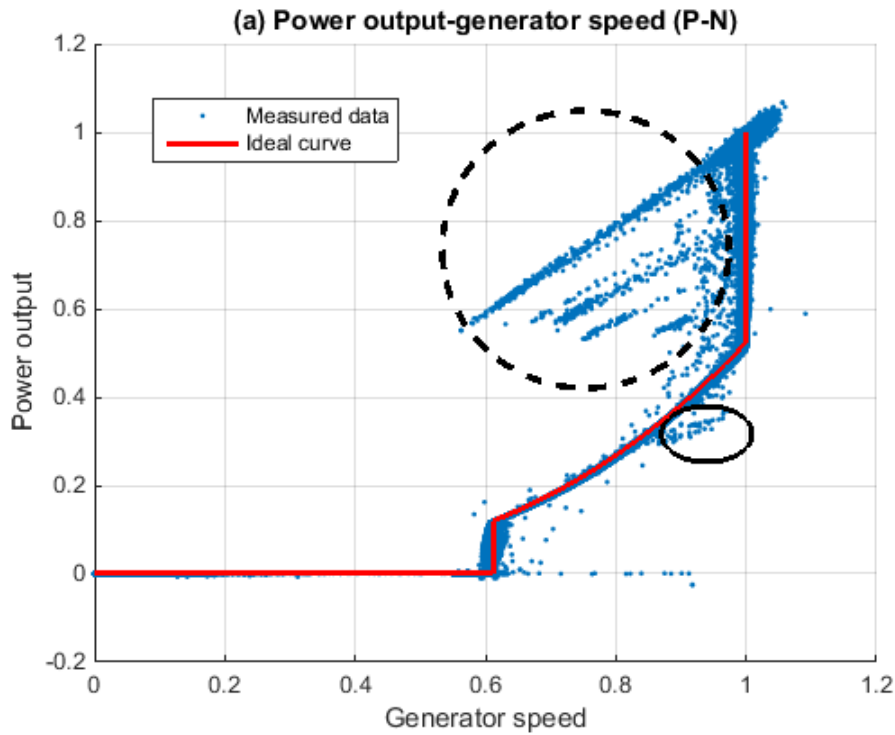
11 Fig. 11. Comparisons of alarms using different CM techniques in Case study 2: (a) the proposed
 12 system; (b) ANN; (c) ANFIS.

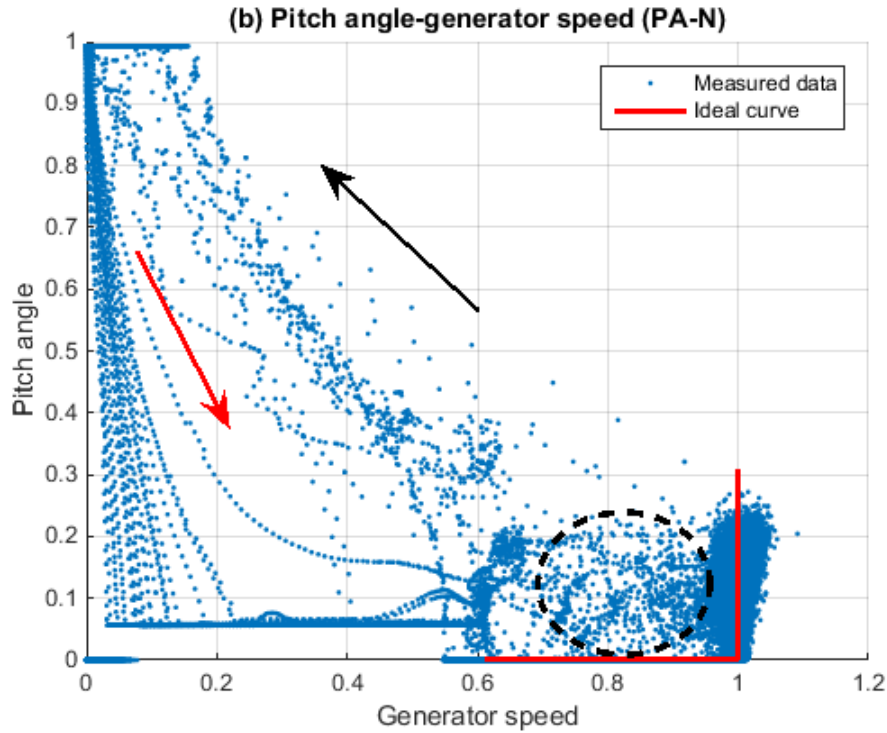
13 *5.3. Case study 3 – pitch controller malfunction of a DFIG-WTG*

14 A WTG alarmed a pitch fault and entered shutdown state at 19:50 on 1/Apr/2015 in the same WF of
 15 Case study 1. Because the wind speed is higher than v_r when the WTG alarm was activated, the
 16 inspection of the pitch system could not be carry out immediately to ensure safety of personnel. The
 17 inspection was carried out and the pitch controller was replaced on 2/Apr/2015.

1 Measured P-N and PA-N curves using SCADA data of the WTG during 27/Mar/2015 to 1/Apr/2015
 2 are illustrated in Fig. 12. During the period, there are 518,400 sets of SCADA data where 893 sets
 3 were regarded as abnormal data which were all due to a pitch controller malfunction.

4 During the first two days, the WTG was shut down and re-operated for several times due to low wind
 5 speed. The pitch angle varied between 0 and 1 unit when the generator speed was lower than the 0.6
 6 of the rated value n_{GCS} . The behaviour of pitch angle follows the red arrow for operation starts and the
 7 black arrow for shutdown processes, as shown in Fig. 12(b). The black circles indicate the abnormal
 8 data in Fig. 12(a) and (b).



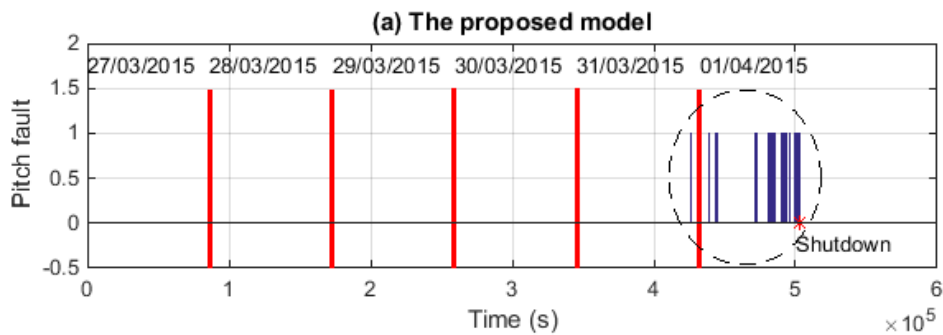


1

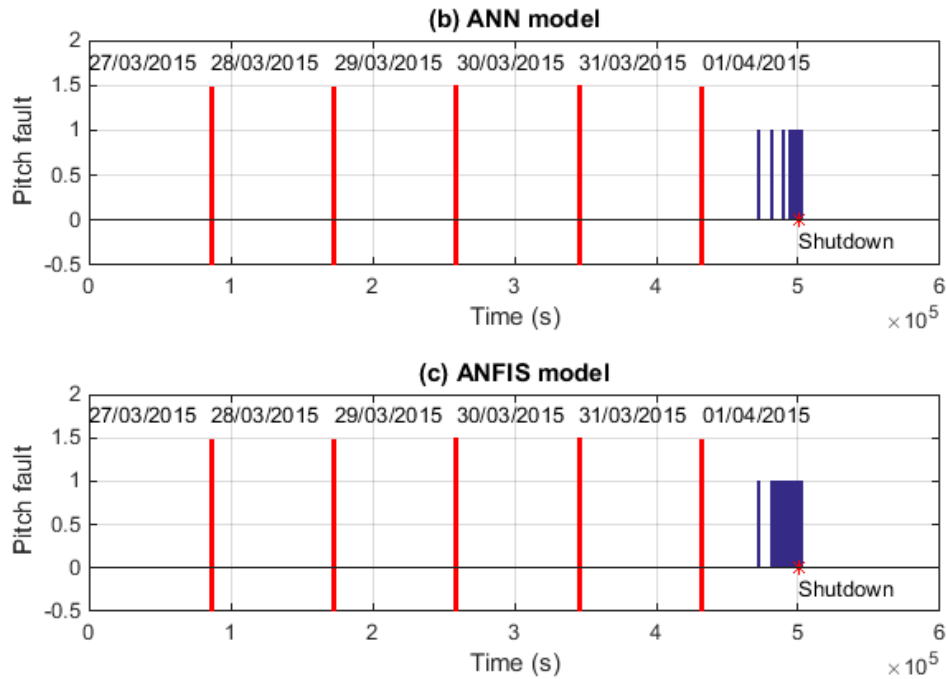
2 Fig. 12. 2D views of selected performance curves in Case Study 3: (a) P-N; (b) PA-N.

3 At 22:28:09 on 31/Mar/2015 the proposed system firstly detected the abnormal data, and as shown in
 4 Fig. 13(a). The abnormal data occurs when the WTG operated under PP1 state and the measured data
 5 deviated from the theoretical curve following Scenario 3. The thresholds of Equation (5.11) were
 6 exceeded, and therefore, the pitch fault was detected. It is seen that the proposed system can detect the
 7 pitch fault conditions nearly 21.4 hours (76,911 seconds) earlier than the existing alarm system. The
 8 ANN and ANFIS models detected the abnormal data 29,476 and 29,484 seconds earlier than the
 9 existing alarm system respectively, as shown in Fig. 13(b) and (c). Therefore, the proposed system is
 10 able to detect the pitch controller malfunction 13 hours (47,427 seconds) earlier than the AI models.

11



12



1

2

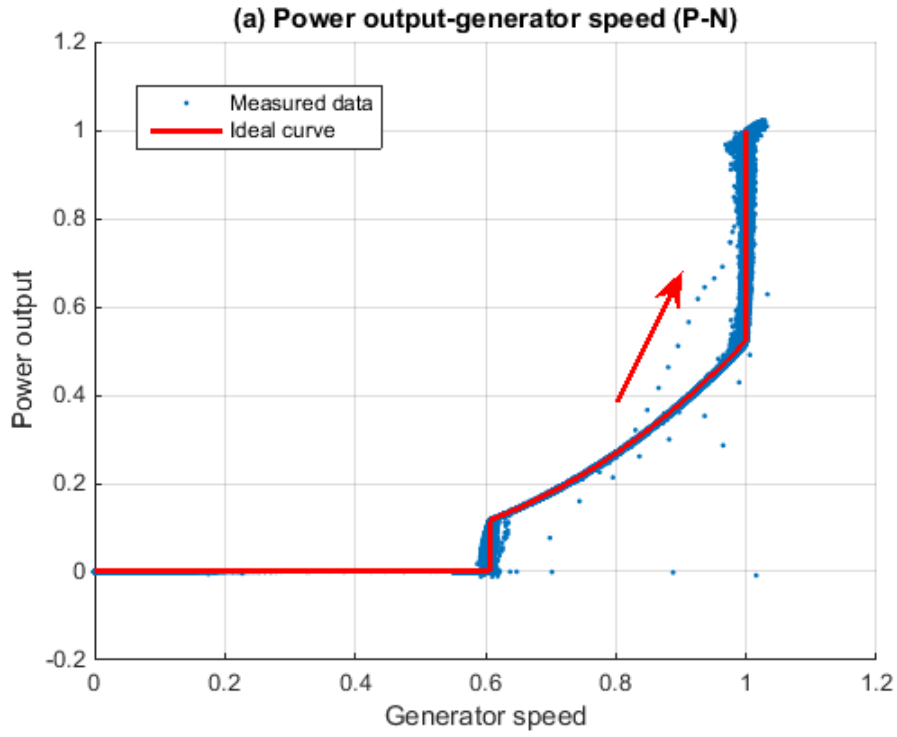
3 Fig. 13. Comparisons of alarms using different CM techniques in Case study 3: (a) the proposed
4 system; (b) ANN; (b) ANFIS.

5 *5.4. Case study 4 – normal operation of a DFIG-WTG*

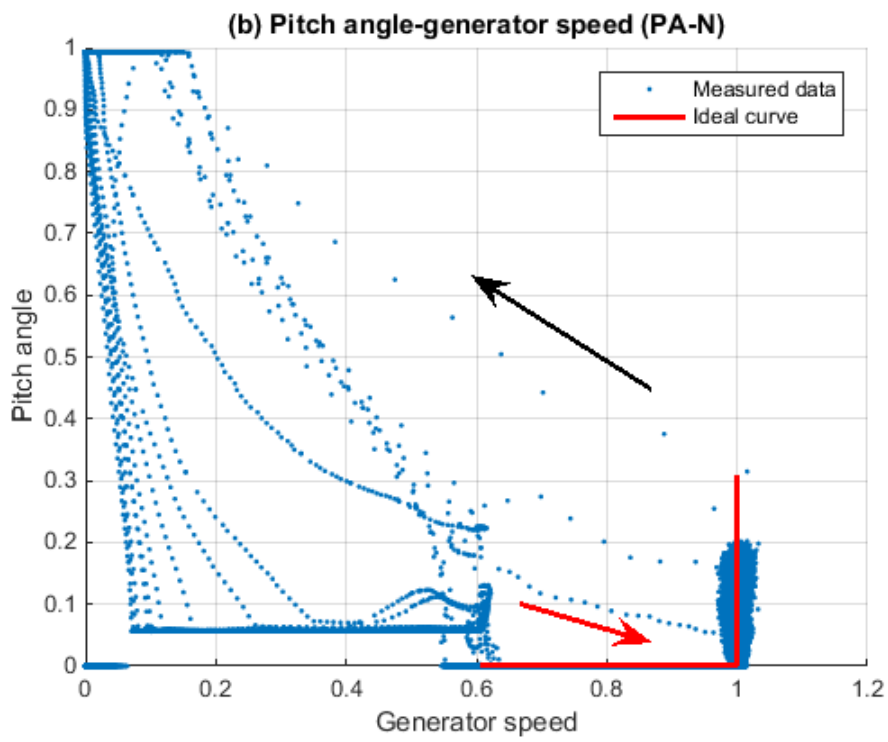
6 Between 02/April/2015 and 05/April/2015, four days' normal operations of a DFIG-WTG are
7 illustrated using 2D views of the selected performance curves, as shown in Fig. 14. There are 345,600
8 sets of instantaneous SCADA data, each set of which includes wind speed, power output, generator
9 speed and pitch angle. It is observed that the Measured P-N and PA-N curves in this period well fit
10 the theoretical curves illustrated in red line.

11 The black arrow and the red arrow respectively illustrate the ES and the stop-to-operation process in
12 Fig. 14(a) and (b). Following the red arrow, the generator speed and power output monotonously
13 increase, and the pitch angle reduces monotonously.

14 This DFIG-WTG has the same configuration and technical specifications as the WTG of Cased study
15 1. Therefore, the PC based NBMs and the relevant criteria apply using the same values of
16 nomenclatures. Fig. 15 shows the results of pitch fault detections by the proposed model, ANN model
17 and ANFIS model. In these processes the deviated data were ignored by the proposed system riding of
18 the false diagnostics using the criteria defined in Equation (9) and (10). No alarm is produced by the
19 proposed system, but the AI models provided alarms on 3/April/2014 and 5/April/2014, because
20 absolute values of prediction errors exceed 100 kW. It is noted that the AI models are trained by
21 SCADA data from the DFIG-WTG. The AI model may accurately predict the power output of the
22 WTG whose operational data are used to model training but failed to provide correct diagnosis in this
23 case. The ANN and ANFIS models respectively produced 4,745 and 5,235 sets of wrong predictions.



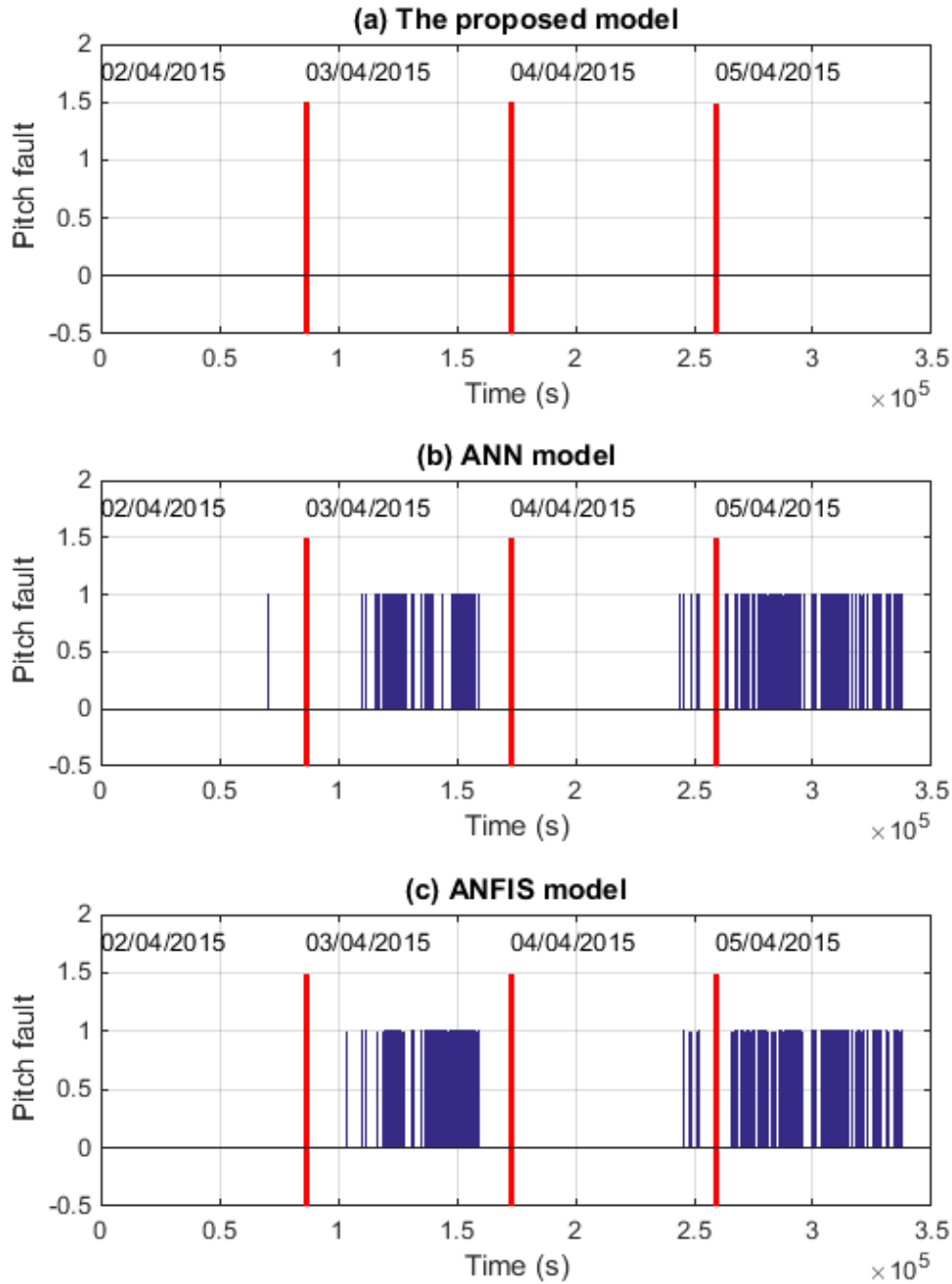
1



2

3 Fig. 14. 2D views of selected performance curves in Case Study 4: (a) P-N; (b) PA-N.

4



1

2

3

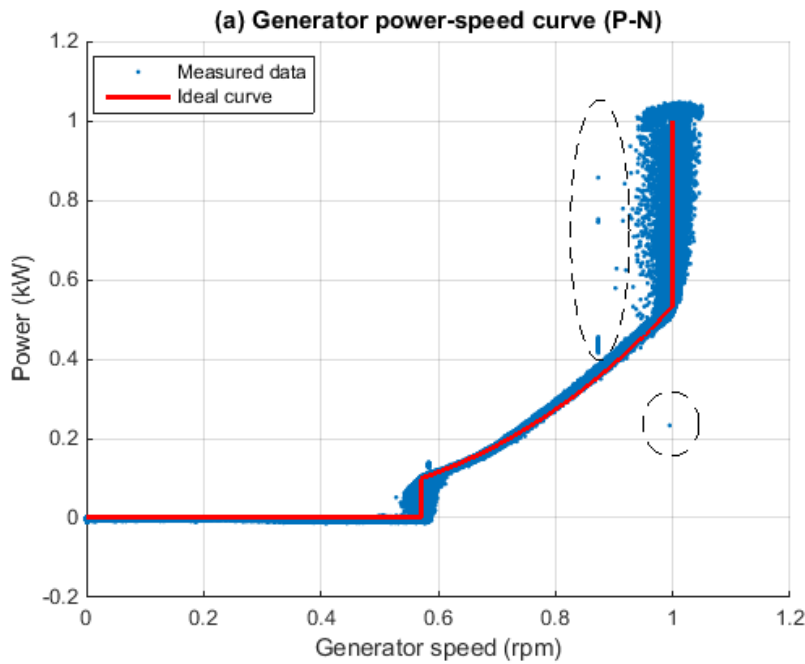
4 Fig. 15. Comparisons of alarms using different CM techniques in Case study 4: (a) the proposed
5 system; (b) ANN; (b) ANFIS.

6 *5.5. Case study 5 – normal operation of a PMSG-WTG*

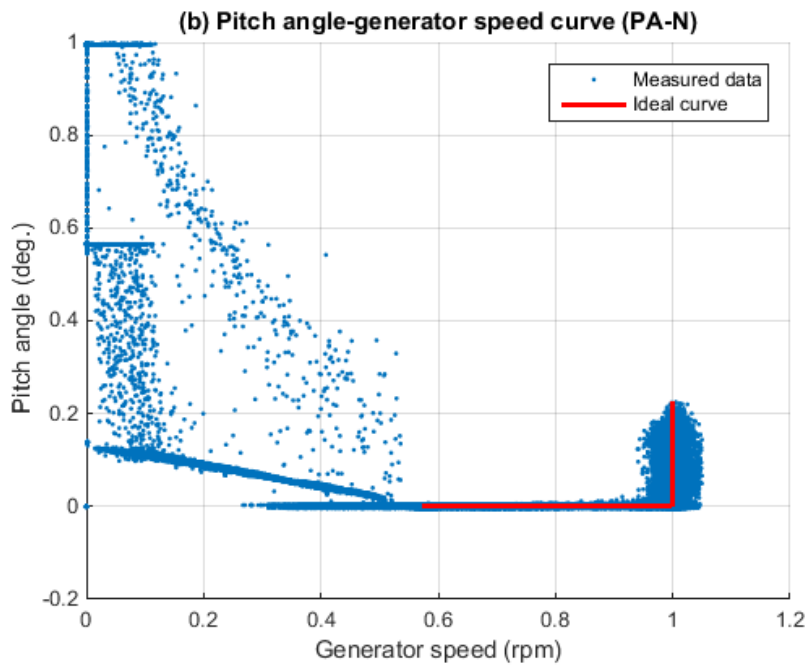
7 Thirty days' normal operations of a PMSG-WTG are illustrated using 2D views of the selected
8 performance curves, as shown in Fig. 16. There are 366,138 (measured every 7 seconds) sets of
9 instantaneous SCADA data, each set of which includes wind speed, power output, generator speed
10 and pitch angle. These data show behaviour of the WTG operating between 31/May/2015 and
11 29/Jun/2015. It is observed that measured P-N and PA-N curves in this period are a good fit to the
12 theoretical curves.

13 Relevant technical specifications of this PMSG-WTG can be found in Table A (CS5). Based on this,
14 the PC based NBMs and relevant criteria can be observed.

1 Fig. 17 illustrates the analysis results of the proposed system, ANN model and ANFIS model. It is
 2 observed that there is no alarm produced by the proposed model. Some points obviously deviated
 3 from the theoretical P-N curve, illustrated in dashed ellipses as shown in Fig. 16(a). However, in PP
 4 states (normalized generator speed is more that 0.6) no abnormal data could be obviously observed in
 5 the 2D view of the PA-N curve, as shown in Fig. 16(b). Due to the fact that only pitching fault data
 6 deviates from both P-N and PA-N curves, these data sets cannot be regarded as anomalies according
 7 to the criteria. In contrast, ANN and ANFIS models detected abnormal data occasionally, as shown in
 8 Fig. 17(b) and (c). The current control system reported no not faults in this period. The ANN and
 9 ANFIS models produced false alarm in this case.



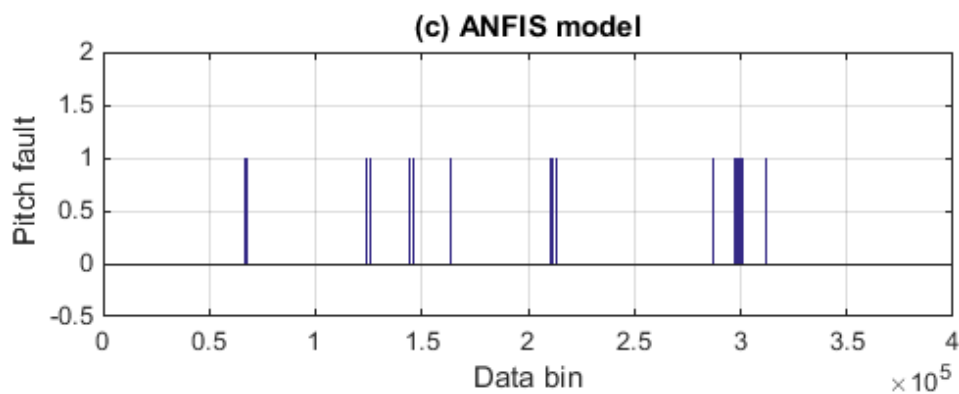
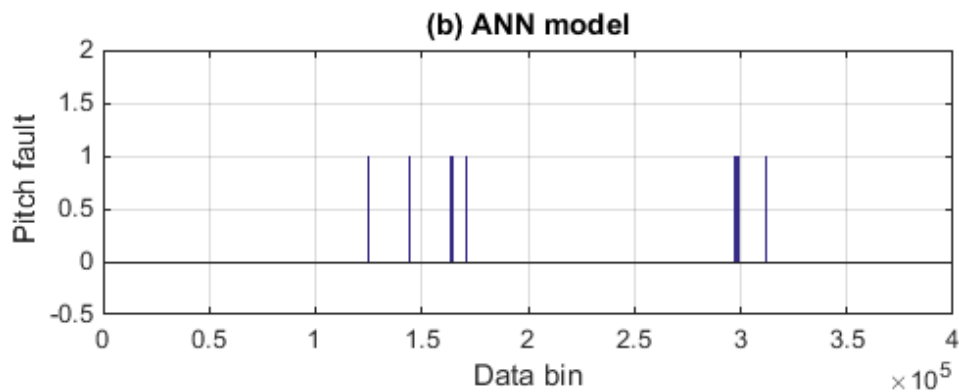
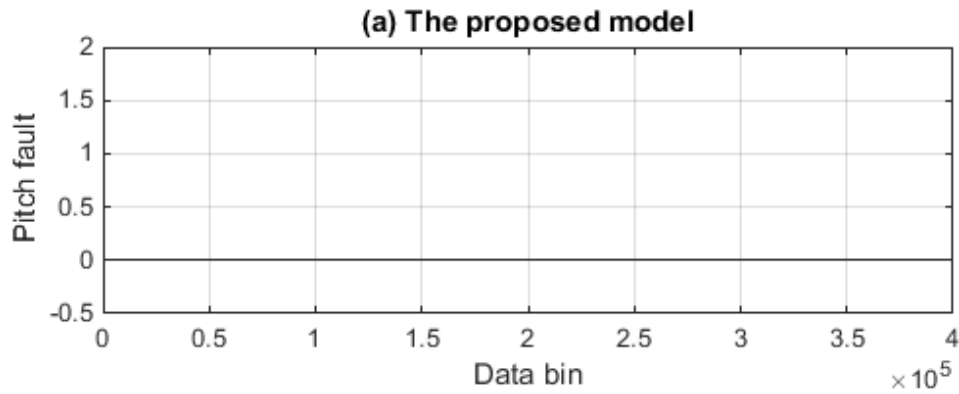
10



11

12 Fig. 16. 2D views of selected performance curves in Case Study 5: (a) P-N; (b) PA-N.

13

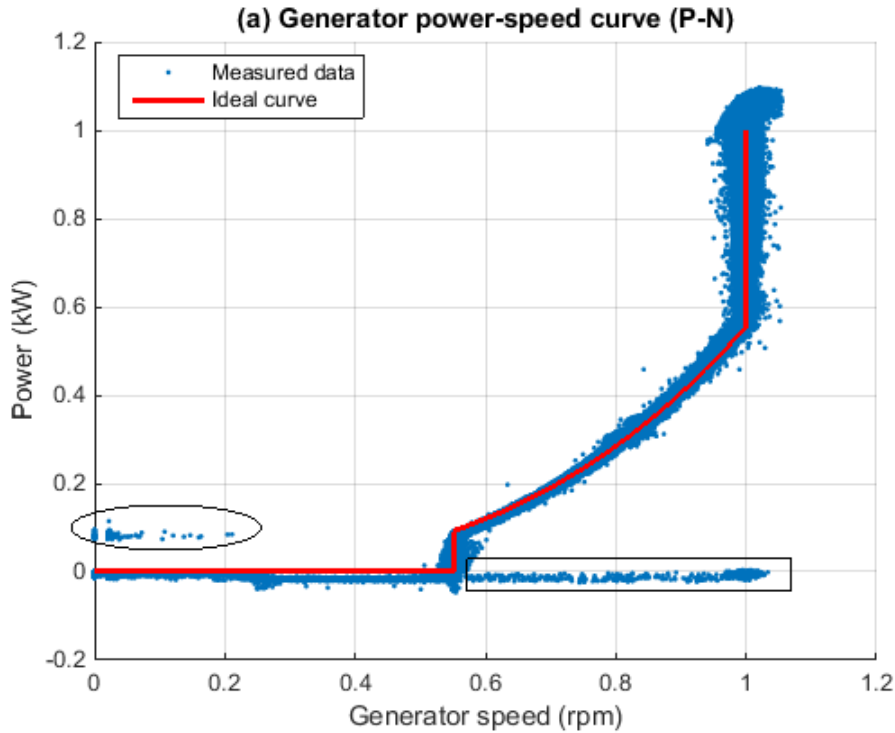


4 Fig. 17. Comparisons of alarms using different CM techniques in Case study 5: (a) the proposed
5 system; (b) ANN; (b) ANFIS.

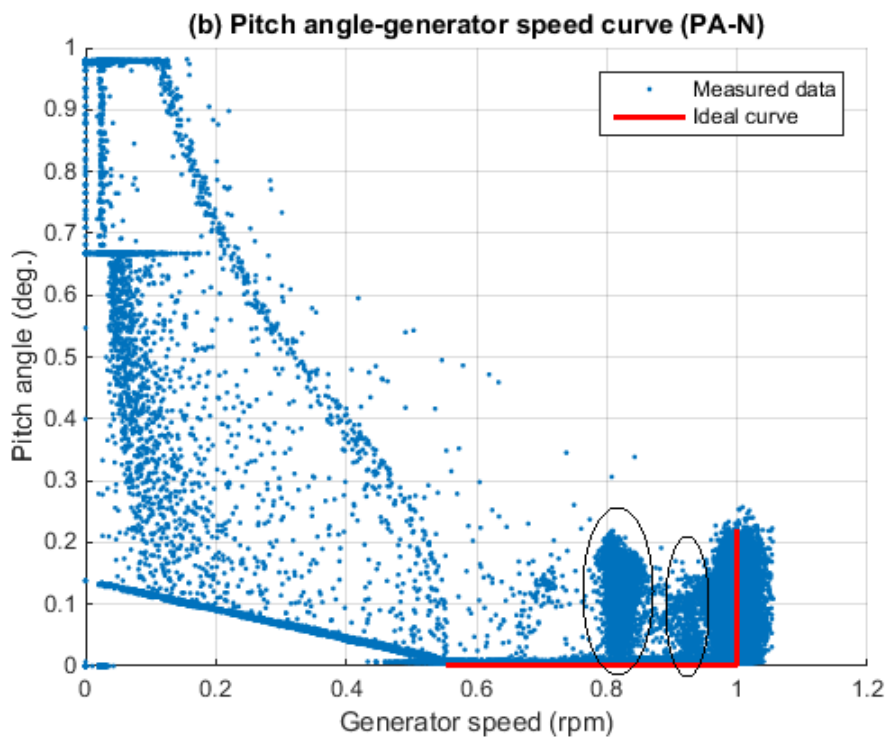
6 *5.6. Case study 6 – normal operation of a PMSG-WTG*

7 On 18/August/2014, the control system of a PMSG-WTG was shut down and reported a series of
8 pitching alarms and nacelle vibration alarms at 1:16 am. After inspection at the site at 9 am, it was
9 observed that one of blades had broken off.

10 The instantaneous SCADA data that was recorded between 3/August/2014 and 18/August/2014 has
11 188,005 sets. Each set of data includes wind speed, power output, generator speed and pitch angle.
12 Fig. 18 illustrates the measured P-N and PA-N curves in this period. The red lines show the
13 theoretical P-N and PA-N curves in the ideal operational conditions.



1



2

3 Fig. 18. 2D views of selected performance curves in Case Study 6: (a) P-N; (b) PA-N.

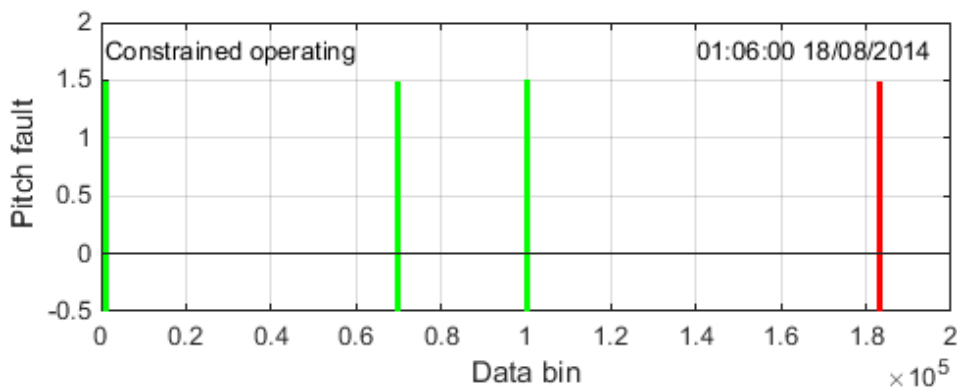
4 In Fig. 18(a), the abnormal data indicated by the ellipse and rectangle deviates from the ideal curve. In
 5 the abnormal data sets, the measured wind speed is in error because the values of measurements are
 6 more than 100 m/s which is far out of the normal range.

7 In the practical operation, the WF operators have to curtail the WTGs' power output if there is a low
 8 grid demand. This manual intervention often results in some WTGs not performing to their factory
 9 supplied specification. An Energy Management System (EMS) was installed in this WF. This system

1 is able to limit the power output of each WTG in the WF to meet the load demand of the network. The
 2 pitch control is used in this constrained operation, as shown in Fig. 18(b). Two ellipses show the
 3 operational data during constrained operation, where the pitch control maintains the generator speed
 4 and power output of the WTG. A mark of constrained operation was recorded by the system to
 5 indicate that this data was recorded when the power output is limited.

6 Relevant technical specifications of this PMSG-WTG are shown in Table A (CS6). Based on this, the
 7 PC based NBMs and relevant criteria can be observed.

8 Fig. 19 illustrates the fault detecting result of the proposed system. There were insufficient WTG data
 9 for model training, and therefore, the AI approaches are not available for comparisons. It is observed
 10 that there is no alarm produced by the proposed model. The constrained operation may mislead the
 11 proposed system to produce false alarms, but the proposed criteria are capable of recognising the
 12 condition. In addition, it is noted that there is no abnormal data on measured P-N curve during the
 13 constrained operation.



14
 15 Fig. 19. Alarms using proposed approach in Case Study 6.

16 *5.7. Discussions*

17 Performance curves are effective tools to study and visualize behaviour of a WTG during operational
 18 conditions with the SCADA data.

19 It is an important advantage of the proposed method that the NBMs and criteria can be obtained from
 20 technical specifications of the WTGs directly and applied on WTG condition monitoring without
 21 model training, the case with AI approaches.

22 Table 1. Comparisons of the proposed techniques and AI approaches for WTG fault detection.

Techniques	Advantages	Disadvantages
PCs	Do not require training models; Can adapt to different WTG concepts.	Knowledge on parameter variances of WTG control and operations.
ANN	Do not require domain knowledge; Easy to apply.	Black-box model; Cannot be interfered.
ANFIS	Can combine experts' experience.	Complicated training processes.

23
 24 The six case studies demonstrate the diagnostic ability of the proposed system for pitch faults of
 25 pitch-regulated WTGs. With scenario 1, 2 and 3 the WTG faults can be clearly identified in 2D view

1 of P-N curves and detected by following the proposed criteria in different operational states in pitch
 2 fault conditions. Pitch fault causes wrong PA-N and P-N relationships, although measurements lie in
 3 their operational range.

4 Table 1 summarizes the advantages and disadvantages among the approaches of performance
 5 curves, ANN and ANFIS. The performance curves allow interpretation of WTGs' behaviours in
 6 different conditions. The domain knowledge of the WTG operations removes the requirement of
 7 model training, and the mathematical model depicting WTG normal operations can be directly
 8 observed using the technical specifications of WTGs.

9

10 **6. Conclusion**

11 The paper proposed NBMs which can be developed using technical specifications of studied WTGs,
 12 and a PC based methodology for making advanced warning of pitch faults caused by pitch controller
 13 malfunction and slip ring pollution. The selected PCs were used to analyse the differences in
 14 behaviour of WTGs from normal operation conditions to pitch fault conditions in six Case studies.
 15 The proposed approach and other AI approaches all are able to detect the anomalies of WTGs earlier
 16 than the existing alarm system. The proposed system is able to detect a polluted slip ring 20 hours
 17 earlier than the AI approaches investigated. The pitch controller malfunctions could be detected by the
 18 proposed approach 13 hours earlier than by the AI approaches. Results demonstrate that the proposed
 19 method is more effective and detect faults earlier than all other approaches.

20 In addition, the proposed approach is able to explain and visualize the abnormal behaviour of
 21 different WTG types during different operational states. Comparing with the AI approaches, the
 22 proposed system will not produce warning in the normal conditions. The proposed approach refers to the
 23 physical characteristics of the WTG and therefore, the system can be directly set up using the
 24 technical specification of the WTG. Each WTG can have a proposed system to monitor its pitch
 25 conditions.

26 **Appendix**

27 Table A. The relevant technical specifications of the studied WTGs in Case Studies (CS).

Parameter	Value			Unit
	CS1	CS5	CS6	
$V_{\text{cut-in}}$	4	3	4	m/s
V_r	10	12	11	
$V_{\text{cut-out}}$	25	22	25	
P_{nr}	1050	750	1125	kW
P_r	2000	1500	2250	
P_{max}	2100	1580	2450	
n_{LPS}	1000	8.8	9.0	rpm
n_{GCS}	1100	9.8	9.8	
n_r	1780	17.3	14.5	
n_{HPS}	1870	19	16	
β_{PL}	0	0	0	degree
β_f	5	-	50	
β_{MO}	25	28	20	
β_{ES}	90	88	90	

28

1 References

- 2 [1] Bi R, Qian K, Zhou C, Hepburn DM, Rong J. A survey of failures in wind turbine generator
3 systems with focus on a wind farm in China. *International Journal of Smart Grid and Clean*
4 *Energy*, 2014; 3(4): 366-73.
- 5 [2] Hameed Z, Hong YS, Cho YM, Ahn SH, Song CK. Condition monitoring and fault detection
6 of wind turbines and related algorithms: A review. *Renew. Sustain. Energy Review* 2009; 13(9):
7 2629-36.
- 8 [3] Hyers RW, McGowan JG, Sullivan KL, Manwell JF, Syrett BC. Condition monitoring and
9 prognosis of utility scale wind turbines. *Energy Mater* 2006; 1(3): 187-203.
- 10 [4] Verbruggen TW. Wind Turbine Operation and Maintenance Based on Condition Monitoring.
11 Final Report Energy Research Centre. The Netherlands, ECN-C-03-047, 2003; 1-39.
- 12 [5] Yang W, Jiang J. Wind turbine condition monitoring and reliability analysis by SCADA
13 information. International Conf. on Mechanic Automation and Control Engineering, Hohhot,
14 China, Jul., 2011; 1872-5.
- 15 [6] Odgaard PF, Stoustrup J, Kinnaert M. Fault tolerant control of wind turbines: a benchmark
16 model. *IEEE Trans. Control Systems Tech.* 2013; 21(4): 1168-82.
- 17 [7] Cross P, Ma X. Nonlinear system identification for model-based condition monitoring of
18 wind turbines. *Renew. Energy* 2014; 71: 166-75.
- 19 [8] Kusiak A, Zheng H, Song Z. On-line monitoring of power curves. *Renew. Energy* 2009; 34:
20 1487-93.
- 21 [9] Sanz-Bobi MA, Garcia MC, Pico JD. SIMAP: Intelligent system for predictive maintenance:
22 Application to the health condition monitoring of a wind turbine gearbox. *Comput. Industry* 2006;
23 57(6): 552-68.
- 24 [10] Schlechtingen M, Santos IF, Achiche S. Wind turbine condition monitoring based on SCADA
25 data using normal behaviour models. Part 1: System description. *Applied Soft Computing* 2013;
26 13(1): 259-70.
- 27 [11] Schlechtingen M, Santos IF. Wind turbine condition monitoring based on SCADA data using
28 normal behaviour models. Part 2: Application examples. *Applied Soft Computing* 2014; 14(1):
29 447-60.
- 30 [12] Chen B, Matthews PC, Tavner PJ. Wind turbine pitch faults prognosis using a-priori
31 knowledge-based ANFIS. *Expert Systems with Applications* 2013; 40: 6863-76.
- 32 [13] Kusiak A, Verma A. Monitoring wind farms with performance curves. *IEEE Trans. Sustain.*
33 *Energy* 2013; 4(1): 192-9.
- 34 [14] Yu Z, Zha X, Wu H. Control of constant rotational speed in wind turbine doubly-fed
35 induction generator system. [Online], Available: <http://www.paper.edu.cn>
- 36 [15] Manwell JF, McGowan JG, Rogers AL. Wind Turbine Control. In: *Wind Energy Explained:*
37 *Theory, Design and Application*, West Sussex, UK: John Wiley & Son Ltd, 2002, p. 321-67.
- 38 [16] *Bladed theory manual*, 4th ed., GL Garrad Hassan, 2010. pp. 46-53.
- 39 [17] Xing G. The application of the similarity law. In: *Fluid Mechanics, Pumps and Turbine*,
40 China Electric Power Press, 2009.

- 1 [18] Johnson KE, Pao LY, Balas MJ, Kulkarni V, Fingersh LJ. Stability analysis of an torque
2 controller for variable speed wind turbines. in *IEEE Conf. Decision and Control*, Atlantis,
3 Bahamas, 2004.
- 4 [19] Bi R, Zhou C, Hepburn DM, Rong J. A NBM based on P-N relationship for DFIG wind
5 turbine fault detection. International Conf. Smart Grid and Clean Energy Technology, Offenburg,
6 Germany, 2015.
- 7 [20] Schlechtingen M, Santos IF, Achiche S. Using data-mining approaches for wind turbine
8 power curve monitoring: A comparative study. *IEEE Trans. Sustain. Energy*, 2013; 4(3): 671-9.

9

10

1



Ran Bi received the B.Sc. degree from the School of Electrical and Electronic Engineering, Huazhong University of Science and Technology, China, in 2011, and the M.Sc. degree in School of Engineering and Computing Science, University of Durham, UK, in 2013.

He is currently pursuing the Ph.D. degree in School of Engineering and Built Environment, Glasgow Caledonian University, UK. His research is mainly focused on SCADA data analysis and WTG condition monitoring.

8

9



Chengke Zhou (SM'13) received the B.Sc. and M.Sc. degrees in Hydropower Automation from Huazhong University of Science and Technology, Wuhan, China, in 1983 and 1986, respectively, and the Ph.D. degree in Electrical Science from The University of Manchester, Manchester, U.K., in 1994.

He joined the School of Engineering and Computing, Glasgow Caledonian University (GCU), in Glasgow, U.K. in 1994 and was a Post-doctoral Research Fellow, Lecturer, and Senior Lecturer until 2006 when he joined Heriot-Watt University as a Reader in Edinburgh, Scotland, UK. In 2007, he returned to GCU as a Professor. He has more than 20 years of research experience in power systems and partial-discharge-based high-voltage plant

19

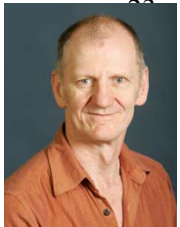
20

21

22

condition monitoring and has acted as a Consultant to EDF Energy, Scottish Power plc, and British Energy. So far, he has published more than 100 papers.

Dr. Zhou is a Fellow of IET and a Chartered Engineer.



Donald M Hepburn (M'08) received his B.A. (Hons) from the Open University in 1987 and the Ph.D. degree from Glasgow Caledonian University (GCU) in 1994. He is a Senior Lecturer at GCU, a member of the IEEE, Institute of Physics, the IET and C.Eng.

He has 20 years of industrial research experience and has been involved in research into HV insulation systems at GCU for over 20 years. His research interests cover monitoring physical and chemical change in HV/MV insulation materials and application of advanced digital signal processing to information from electrical, acoustic and RF monitoring techniques.

31